UNIVERSITA' DEGLI STUDI DI PADOVA
DIPARTIMENTO DI INGEGNERIA DELL'INFORMAZIONE
CORSO DI LAUREA MAGISTRALE IN BIOINGEGNERIA

TESI DI LAUREA

A magnet-compatible isometric handgrip protocol with real-time visual feedback for coronary endothelial function MRI assessment

---

RELATORE INTERNO
Prof. Alfredo Ruggeri

RELATORI ESTERNI
Prof. Matthias Stuber
PhD Jerome Yerly
MSc Giulia Ginami

LAUREANDA
Giovanna Nordio
Matricola: 1041029

14 Ottobre 2014
Anno Accademico 2013-2014

A papa', mamma e Andy

Abstract

Cardiovascular diseases are the major cause of death in the western world; among them, coronary artery disease (CAD) has the biggest impact in terms of mortality of the population.
The endothelium is the major regulator of vascular homeostasis, since it preserves the correct balance between vasodilatation and vasoconstriction of the vessel wall. An alteration of its functionality could have serious consequences in the correct functionality of the coronary arteries. The arterial wall can be damaged and atherosclerotic plaques start to form on the vessel wall, increasing the vessel wall thickness. When the plaques are unstable or obstructive, they lead to ischemic syndromes, which are the clinical manifestation of atherosclerosis and CAD. For these reasons, it is important to develop a tool that is clinically applicable and reliable, and allows a non-invasive assessment of the endothelial function in order to eventually predict plaque formation. Magnetic resonance imaging (MRI) is promising potential solution in this scenario, since it allows non-invasive acquisition of anatomical and functional information of the coronary artery. In addition, stress tests are a useful modality to discriminate normal from abnormal cardiovascular function. In this master thesis work, a new and robust set-up has been developed, which combines MRI with an isometric handgrip exercise to perform stress tests. Several studies have used an analog ergometer, but it has severla major drawbacks: it induces eddy currents, the subject has to lie in prone position during the scan, and direct external supervision is required to verify proper grip strength. To overcome these drawbacks, the work in this thesis uses a digital handgrip that facilitates patient compliance during the experiment. Eddy currents are avoided and the subject can lie in a more comfortable supine position. The digital ergometer is integrated with a real-time feedback of user's grip strength; thanks to that, direct external supervision is not needed anymore. The set-up is validated with data acquisition in healthy volunteers. The images are acquired before and after the stress test, and the differences in the vasodilatation and lumen diameter of the vessels are investigated between the two acquisitions.
Two different techniques of image acquisition are tested, the *Restrospective ECG-gated cine technique* and *the Retrospective self-gated cine technique*. The images are reconstructed using *Compressed Sensing* (CS) technique, which permits the acquisition of less data thus reducing the scan time.

Keywords: CAD, endothelial function, coronary MRI, digital isometric handgrip exercise, CS

Prefazione

Le malattie cardiovascolari sono la prima causa di morte nel mondo occidentale. Ad essere colpite sono soprattutto le arterie coronariche, vasi sanguigni destinati all' irrorazione del cuore; una loro ecclusione può causare infarto miocardico e in casi estremi il decesso.
Il tessuto endoteliale delle arterie coronariche è il principale regolatore dell' omeostasi vascolare, poichè mantiene il giusto equilibrio tra vasodilatazione e vasocostrizione del vaso sanguigno. Se la funzione endoteliale viene alterata, ci possono essere severe conseguenze sulla corretta funzionalità delle arterie coronariche. Sulla parete all'interno del vaso sanguigno si formano delle placche aterosclerotiche, le quali contribuiscono ad aumentare lo spessore della parete alterando il normale fluire del sangue. Quando le placche diventano instabili e bloccano il flusso sanguigno, si hanno fenomeni ischemici, prima manifestazione di aterosclerosi.
E' quindi di fondamentale importanza avere a disposizione un possibile strumento clinico che permetta di investigare in modo non invasivo la funzione endoteliale delle arterie coronariche al fine di prevenire la formazione di placche aterosclerotiche. La risonanza magnetica permette di ottenere informazioni anatomiche e funzionali delle arterie coronariche in modo non invasivo. Affiancando alla risonanza magnetica un esercizio di stress fisico è possibile discriminare un normale da un anomalo funzionamento cardiovascolare.
In questo lavoro di tesi magistrale è stato implementato un nuovo e robusto set-up che combina la risonanza magnetica con un esercizio di stress fisico utilizzando un dispositivo di handgrip digitale. In precedenti studi e' stato utilizzato un handgrip analogico, il quale ha però diversi aspetti negativi: l' handgrip induce *eddy currents* quando inserito all' interno dello scanner, il volontario deve distendersi prono durante l'esame di risonanza magnetica, e per tale motivo è necessaria una supervisione esterna da parte di un infermiere al fine di monitorare l'effettiva forza esercitata dal volontario con l' handgrip.
Il set-up proposto sostituisce l' handgrip analogico con un handgrip digitale al fine di superare tali limitazioni e di facilitare l' esecuzione dell' esercisio di stress fisico all' interno dello scanner da parte del volontario. Diversi sono i vantaggi introdotti dall' handgrip digitale: non è più affetto da *eddy currents* e il volontario puo' quindi distendersi in posizione supina all' interno dello scanner. L' handgrip digitale è integrato con un *real-time visual feedback*, che mostra in tempo reale al volontario la forza esercitata con l'handgrip. Grazie a questo sistema visivo non è più necessaria la presenza di una persona che legga i valori di forza esercitati dal volontario. Il set-up implementato è stato testato e validato su volontari sani. Le immagini delle arterie coronariche sono state acquisite prima e successivamente l' esecuzione dell' esercizio fisico con handgrip, al fine di poter visualizzare una dilatazione delle arterie coronariche tra le due acquisizioni. Sono state utilizzate due tecniche di acquisizione, la *Retrospective ECG-gated cardiac cine imaging* e la *Retrospective self-gated cardiac cine imaging*, e le immagini ottenute sono poi state confrontate. Le immagini sono state successivamente ricostruite con la tecnica di *Compressed Sensing*, la quale permette di acquisire le immagini partendo da un numero inferiore di dati riducendo così il tempo totale necessario per un esame di risonanza magnetica.

Table of contents

List of Figures

List of acronyms and abbreviations

CAD	Cardiovascular Artery Disease
CVD	Cardiovascular Disease
MRI	Magnetic Resonance Imaging
LDL	Low-Density Lipoprotein
NO	Nitric Oxide
ECG	Electrocardiography
GUI	Graphical User Interface
CS	Compressed Sensing

Introduction

This master thesis proposes a new non-invasive set-up for coronary endothelial assessment in coronary artery disease. This first chapter is a summary of the whole work, presenting coronary artery disease and its worldwide impact, the state-of-the-art and the limitations of the previous imaging techniques used for coronary endothelial assessment, the hypothesis behind this work and the solution proposed. The main goal of the thesis is then clearly defined in the second section, while the last section presents the structure of the thesis.

1.1 Introduction

Diseases of the heart and circulatory system, called cardiovascular disease (CVD), are the main cause of death both in Europe and United States. Among all CVDs, the coronary artery disease (CAD) is the leading cause of cardiovascular mortality worldwide. It is a vascular disorder that manifests with a chronic progression of plaques formation on the vessel wall, causing an increase of its thickness and endothelial dysfunction. These plaques or atherosclerotic lesions can become unstable and occlude the vessel lumen, which can lead to ischemic syndromes and in severe cases, to death.[1]
In 1996, 29% of worldwide mortality was due to CVD and CAD was estimated to have caused half of these deaths.[2] Recent statistics in the United States show a rapid and evident increase of deaths attributable to CVD (Figure 1).[3] CVD is also the main cause of death in the European Union (EU), with 1.9 million of death each year.[4]

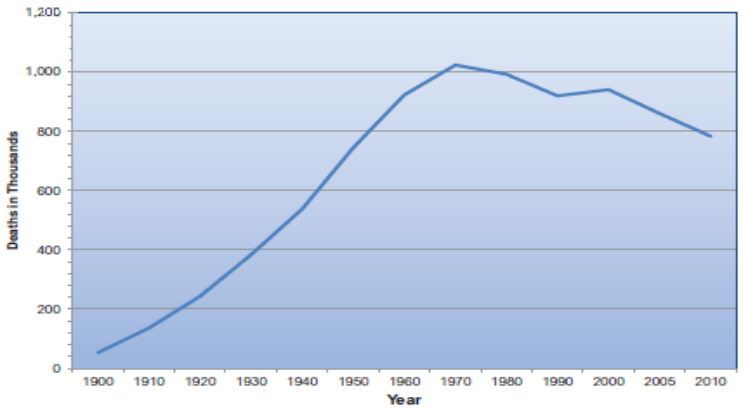

Figure 1: Deaths attributable to cardiovascular disease (United States: 1990-2010). Cardiovascular disease (International Classification of Diseases, 10th Revision codes I00-I99) does not include congenital. Before 1933, data are for a death registration area and not the entire United States. Source: National Center for Health Statistics. The graph is reproduced from reference [4].

The developing countries are an interesting example, where the CAD mortality has consistently increased in the last years. It has been estimated that, by 2020, CAD will be the largest cause of death in these countries (Figure 2). [2] This statement is motivated by the rapid spread of the main risk factors of CAD, such as diabetes, smoking, hypertension and hypercholesterolemia. This rapid spread is mainly due to globalization and urbanization, which make CAD an epidemic.

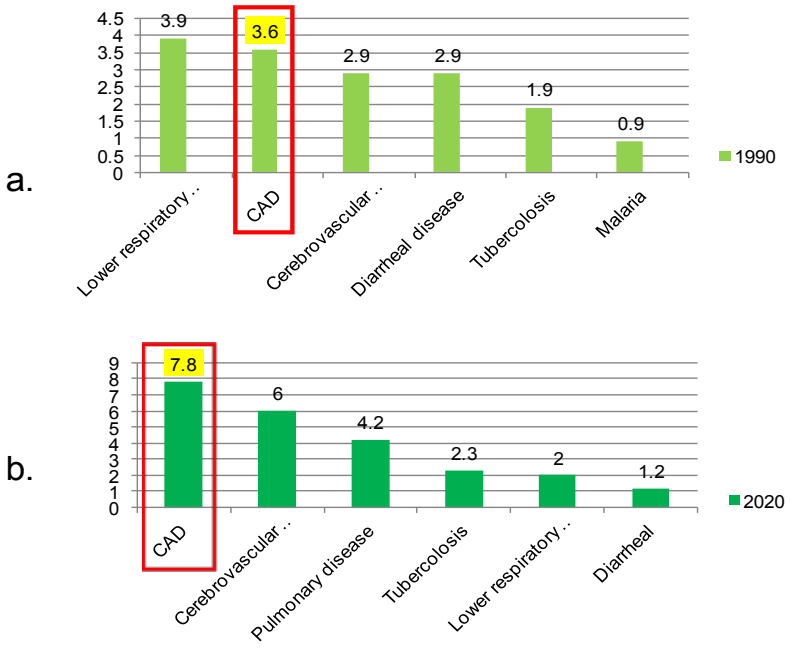

Figure 2: (a) Leading causes of death in developing countries in 1990 and (b) projections for 2020. The x-axis shows the causes of death and the y-axis the number of death (in millions). The graph is reproduced from the article of Karen Okrainec et al. [2]

The worldwide impact of CAD does not only regard the number of death, but also the healthcare and economic burden; CAD is in fact becoming the major public health problem with significant heavy economy costs. In 2003, it has been calculated that CAD has cost the EU €45 billion [5], while in the United States the number of cardiovascular operations and procedures have increased from about 6 millions in 2000 to about 7.5 in 2010 [3]. These data underline the importance to investigate and study potential predictors of CAD in order to reduce the risk of future coronary events and find possible prevention therapies for these diseases.

First of all, it is important to analyse the pathophysiology of CAD, in order to better understand where and how to intervene to reduce the worldwide impact of this disease. Coronary atherosclerosis manifests with the formation of plaques on the vessel wall. These plaques can silently accumulate, reducing the vessel lumen, and in severe cases they can completely occlude the vessel. Unstable plaques can eventually rupture and cause thrombosis or embolism.[6] The chronic progression of CAD is associated with an alteration of the endothelial function, which means that the atherosclerosis lesion reduces the vasomotor response of the endothelium.[7] The coronary endothelial function (CEF) can then be considered as one of the main markers of atherosclerosis and its earlier investigation could give important information about the progression of CAD in patients.

Different imaging techniques have been proposed to assess the endothelial functionality, including ultrasound and angiography. Ultrasound is a non-invasive technique that processes the reflected oscillating sound pressure wave to create an image of the coronary artery and the plaques, while coronary angiography is an invasive technique that uses x-rays and contrast agent to visualize the lumen of the coronary artery.[8] However both of these techniques have some drawbacks that have limited their clinical use. Ultrasound is subject to low image quality that is highly operator dependent, whereas angiography employs potentially harmful ionizing radiation and iodinated contrast agent. Instead, the ideal imaging modality should be clinically reliable, without entailing any problems on the final diagnosis, while preserving image quality. Simultaneously, the imaging technique needs to be completely safe for the patient.

It is thus necessary to find an alternative imaging technique to assess the endothelium of the coronary artery. Magnetic Resonance Imaging (MRI) is an innovative, non-invasive technique for coronary imaging, which has gone through considerable development and improvements in the last years. MRI is a completely safe technique for the patient, which allows coronary vessel wall and plaque imaging.[9] It is then interesting and challenging to use MRI in order to assess CEF, namely the vasomotor response of coronary artery. To achieve this, an additional observation has to be done.

In general, in response to a stress test, the vessel dilates, causing an increase in cross sectional area and blood flow. A correct or incorrect vasomotor response of the coronary artery can then be assessed by acquiring cross sectional images of the coronary artery before and after inducing a dilatation of the vessel with a stress test. In order to assess CEF, in this work MRI is combined with an isometric handgrip exercise. Until now an analog handgrip has been used, but it has several major drawbacks when used in a MR scanner: the eddy currents induced by the magnetic

field cause the device to vibrate, the subject needs to lie prone in the scanner [10-13] and an external observer is required to continuously monitor the subject's grip strength. I hypothesize that substituting the analog ergometer with a digital one can solve these problems and improve the assessment of CEF.
A new set-up for the isometric digital handgrip exercise combined with MRI was developed, implemented, and tested on healthy volunteers. The digital ergometer is integrated with a real-time visual feedback of the user's grip strength. CEF is assessed by measuring the cross sectional area of the coronary artery before and after the stress test. With this innovative set-up the limitations of the analog handgrip would be addressed, providing a more comfortable environment for the performance of the exercise.
The future clinical use of this set-up in order to assess CEF could have a considerable impact on the healthy and economy worldwide, since it could be used as a potential instrument to diagnose and monitor the progression of CAD.
The images are acquired with a 3T scanner (MAGNETOM Prisma, Siemens Helathcare) and then reconstructed with Compressed Sensing (CS) technique. Generally cardiac MRI needs a continuous measurement of the ECG, in order to gate or synchronize it together with the image acquisition and to reduce cardiac motion artefacts. However, retrospective ECG gating techniques are vulnerable to arrhythmias and the ECG signal is not always available because of RF interference and patient electrophysiology. Therefore, instead of using a Retrospective ECG gating technique to reconstruct the image, in this work a self-gated approach will be used.

1.2 Thesis purpose

The main goal of this thesis is to develop, implement, and test a new and innovative method to assess CAD, in particular CEF, in a non-invasive way. The method could then be used in clinic to monitor the progression of the coronary calcification, since an earlier investigation of CAD could prevent severe future development of the disease. Since the worldwide significance of CAD is more and more increasing, the advantages eventually introduced would have then an important impact on the healthcare and economy.
A new set-up for MRI combined with isometric handgrip exercise is then implemented. The analog ergometer, previously used, is substituted with the digital one. Since the digital ergometer has not any panel on which the grip strength of the volunteer can be displayed, a real-time visual feedback is built and integrated within the set-up. The set-up is then tested on healthy volunteers in order to verify its features. The main goal of this set-up is to assess CEF, by evaluating the vasomotor response of the coronary artery after a stress test. Measurements of the cross-sectional area of the coronary artery are done on the images acquired before and after the isometric

handgrip exercise. The efficacy of the isometric handgrip exercise should induce a vasodilatation of the coronary artery in response to the stress test.
Since by using the retrospective ECG-gated technique the ECG signal is not always available, the images are acquired and reconstructed using a self-gated approach together with the compressed sensing technique. With this new approach it is possible to reconstruct the images based on a correlation self-gated signal built after the data acquisition.

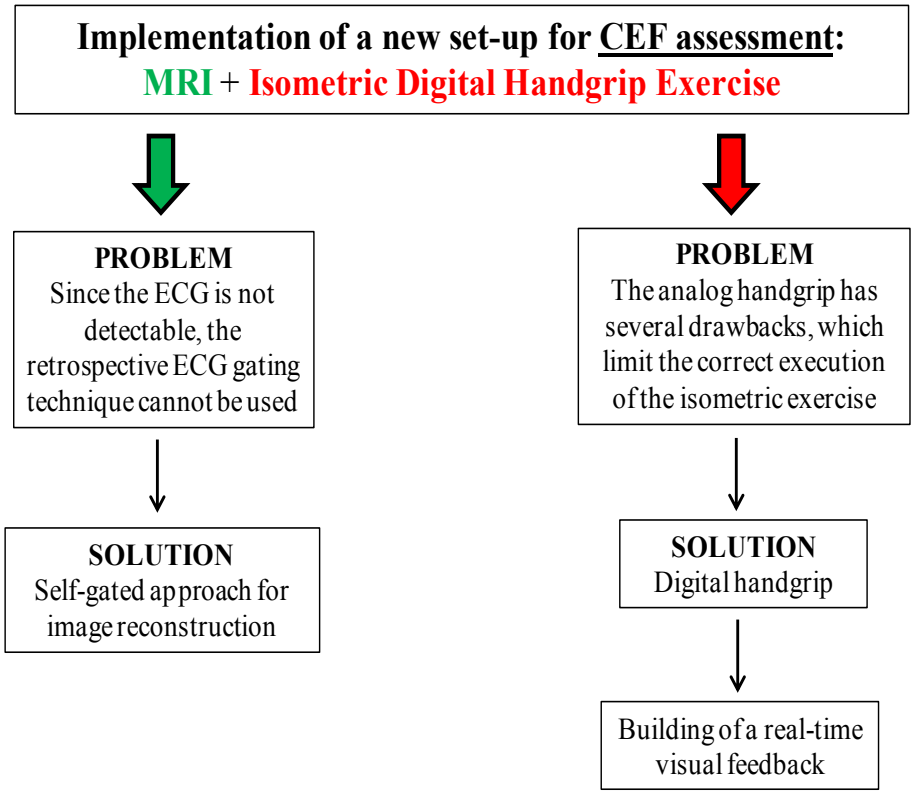

1.3 Structure of the thesis

The thesis is structured as followed:

- ***Chapter 1 - Introduction***
  In the first chapter, a general overview of the whole work is given to the reader. CAD is an important disease with a notable worldwide impact on the healthcare and economy. It is thus important to find a possible method in order to investigate, predict and monitor CAD. The main purpose of the thesis is then presented: the implementation of a new set-up for non-invasive CEF assessment, by combining MRI with isometric digital handgrip exercise. Problems and possible solutions to reach the main goal are outlined.

- ***Chapter 2 – Background***
  The reader needs to first of all understand what CAD means in order to further completely follow the work. The main features of CAD are explained together with the important role played by the endothelium. The second section of this chapter consists more on a technical background, focusing on imaging techniques, in particular on coronary MRI. The role of isometric handgrip exercise is then presented, briefly introducing the previous results obtained with the analog handgrip.
- ***Chapter 3 – Methods***
  Several methods have been implemented and used in this thesis, which are presented and explained in this chapter. The set-up for CEF assessment is developed using MATLAB program, in order to build the real-time visual feedback and to digitally record the handgrip strength data. The protocol for data acquisition, the self-gated approach and the image reconstruction techniques are then explained.
- ***Chapter 4 – Analysis and Results***
  The results obtained using the implemented real-time visual feedback are presented in this chapter. First, the results of the survey about how the volunteers performed the isometric handgrip exercise are presented. Next, I analyze if it is possible to detect a vasodilatation of the right coronary artery after the stress test, by measuring the cross-sectional area of the vessel. The images are acquired using two different techniques. The differences, advantages and disadvantages of these techniques are analysed and compared. Finally, I present and analyze the results of the linearity test of the handgrip device.
- ***Chapter 5 – Conclusion and Future Work***
  In conclusion in this chapter the results obtained are discussed, future works are proposed and final reflections regarding the possible impacts of the proposed works are done.

2 Background

This chapter first introduces some of the fundamental physiological and pathophysiological concepts underlying the work in this thesis. I first review the normal anatomy and physiology of the heart and coronary arteries, and then present atherosclerosis and coronary artery disease. The second section of this chapter describes techniques to image the coronary arteries and assess the coronary endothelial function using isometric handgrip exercise.

2.1 Clinical background

The heart is a pump that delivers blood and nutrients to the organs and cells of the human body. Because the heart is a muscle itself, it also needs oxygen and nutrients to function. This supply of blood and oxygen is ensured by the right (RCA) and left (LCA) coronary arteries. These arteries originate from the root of the aorta, immediately above the aortic valve, and they course along the pericardial surface. They divide in progressively smaller vessels, arterioles and then capillaries, to deliver oxygenated blood to the heart's cells. The right coronary artery supplies the right side of the heart, while the left coronary artery supplies the left side of the heart, which is generally bigger and more muscular (Figure 3).

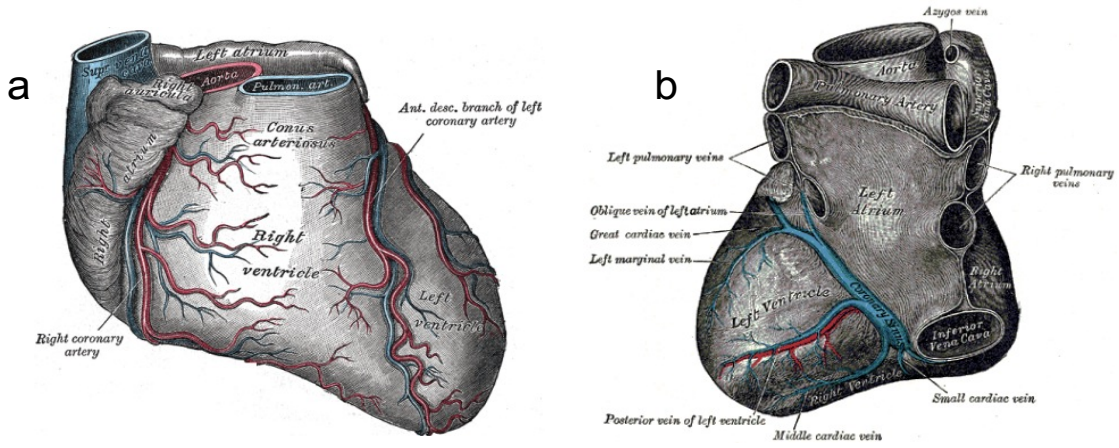

Figure 3: Sternocostal (a) and diaphragmatic (b) surface of the heart. The RCA and LCA originate from the right and left aortic sinus, respectively. The coronary arteries are shown in red (a) while the coronary sinus is shown in blue (b). Image from reference [14].

A blood vessel is composed of three layers: the intima, the media, and the adventitia (Figure 4). The intima is the innermost layer that has a thin layer of endothelial cells lining the interior surface of the vessel wall, known as the endothelium. The endothelium acts as a semi-selective barrier that controls the exchange of materials with the white blood cells. Another function of the endothelium is to regulate vascular homeostasis and to maintain normal vascular tone (contraction).

The media is the middle layer in arteries composed of smooth muscle cells and other extracellular components. The smooth muscle cells can contract (vasoconstriction) or relax (vasodilatation) to control blood flow in response to physiological stimuli. These muscles control autoregulation of blood supply in order to maintain a steady blood flow at the capillary level.

The adventitia is the outermost layer of the blood vessel that contains connective tissue to attach the vessel to the surrounding tissue, such as muscles.

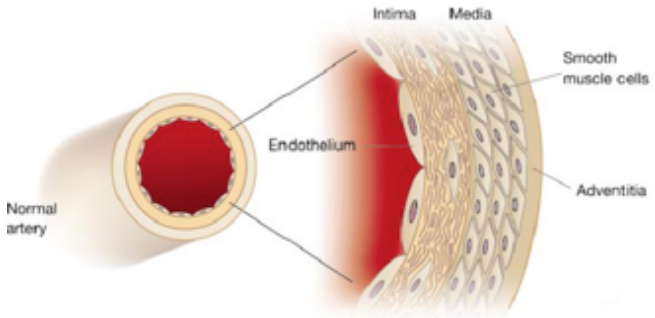

Figure 4: The normal human coronary artery has a trilaminar structure. The endothelium is the thin layer of cells that covers the inner surface of the vessel wall. The intima contains the smooth muscle cells scattered within the intimal extracellular matrix, while the media contains of different layers of smooth muscle cells in a matrix containing both elastin and collagen. Image from reference [15].

A healthy endothelium controls vascular function by responding to various hormones, neurotransmitters, and vasoactive factors. Disruption of this normal vascular function can lead to the development of atherosclerosis and subsequently life-threatening cardiovascular problems. The following section provides a brief review of atherosclerosis, which is one of the most common cardiovascular diseases.

2.1.1 Pathophysiology of atherosclerosis

Atherosclerosis is an inflammatory disease characterized by an increase of the vessel wall thickness due to the accumulation of lipids within the vessel wall, known as plaques. The early signs of atherosclerosis already manifest during childhood and adolescence as fatty streaks in the artery wall. In advanced staged of the disease, these plaques can rupture and may cause stroke and/or myocardial infarction.

The low-density lipoproteins (LDL) are one of the five groups of lipoproteins that enable the transportation of lipids, such as cholesterol, within the water around the cells. In atherosclerosis, the level of LDL inside the vessel increases. The LDL is then transformed by enzymes into proinflammatory particles, which activate the innate inflammatory system in the intima. The inflammation starts when the endothelial cells are activated and secrete adhesion molecules that will attract monocytes, lymphocytes and mast cells into the arterial wall. The monocytes then differentiate into macrophages, which metabolize the lipids before becoming foam cells. This step plays a crucial role in the later development of the lesions, since the death of macrophages and the accumulation of necrotic debris provoke further inflammation. Consequently the normal shape of the artery begins to be altered, due to the accumulation of lipid pools in the central part of the intima. The fibrous tissue is added to the necrotic debris forming a fibrous cap. The accumulation of degenerative material inside the vessel lumen is called atheroma. [6, 15-18]

At the early stage of the disease, there is a phenomenon of compensation or positive remodelling to preserve the vessel lumen, *i.e.* the arterial wall enlarges its diameter to compensate for the lesion growth. This process continues until the enlargement of the wall can no longer compensate for the lesion growth, at which point narrowing of the vessel lumen becomes visible. Narrowing of the lumen can cause severe hemodynamic effects and potentially block the blood flow (Figure 5).[6] But more often, the fibrous cap can become thin and weak, making the plaque vulnerable to rupture.

The main consequences of a plaque rupture inside the coronary artery are thrombosis and embolism. The thrombosis manifests when the plaque content comes in contact with the blood, which causes the formation of a thrombus, *i.e.* a blood clot constituted by fibrin and blood cells, and obstructs the blood flow through the vessel. The thrombus can sometime break loose and get carried downstream to plug another smaller vessel causing thromboembolism. A severe and extreme blockage of the vessel in both cases can cause myocardial infarction. Possible symptoms of these diseases are chest pain, weakness, and difficulty to breath. [19]

Beyond that, there are other important risk factors that can accelerate and accentuate the development of future atherosclerosis, such as smoking, diabetes and hypercholesterolemia.[6]

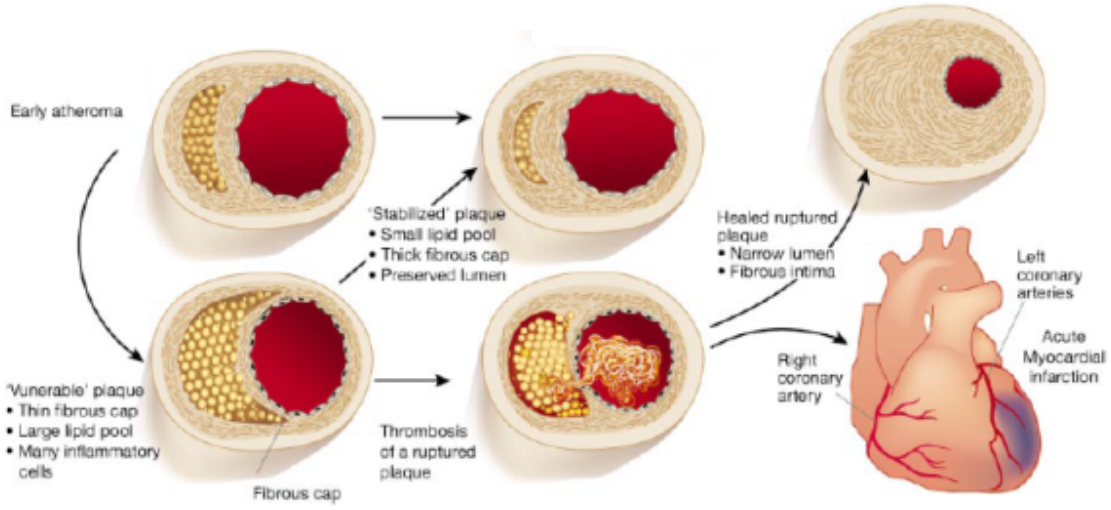

Figure 5: Schematic of the life history of an atheroma. Two possible progressions can then happen: on one side the plaque can stabilize, on the other hand it can rupture and cause thrombosis. At the beginning there is a phenomenon of compensation or remodelling, but when the plaque occupies the 40% of the total area of the artery serious complications appear [6]. Image from reference [15].

2.1.2 Endothelial function in coronary artery disease

The progressive development of atherosclerosis is related to the inflammation. In fact, the early stability of the plaques is then permanently altered by the cellular infiltration inside the cap, in particular the infiltration of inflammatory cells.[20]
Together with the inflammation, the endothelial function plays a crucial role in the development of atherosclerosis, and in general of coronary artery disease. The endothelium monitors the vascular homeostasis by the secretion of both vasodilators and vasoconstrictors. Nitric oxide (NO) is the major vasodilator secreted by the endothelium, which controls the vasodilatation, inhibits the inflammatory response and suppresses the growth of smooth muscle cells. On the other hand vasoconstrictors, such as endothelin and angiothensin II, are secreted in order to stimulate the production of smooth muscle cells. The correct functionality of the endothelium balances the secretion of both vasoconstrictors and vasodilatators. If this equilibrium is unbalances and an incorrect production or activity of NO occurs, then the functionality of the endothelium is altered.
Because of the important role of the endothelium, an alteration of its structure and function can have severe consequences in the development of CAD. By constantly monitoring the

functionality of the endothelium, it is possible to have direct information about the progression of the disease (Figure 6).[7]

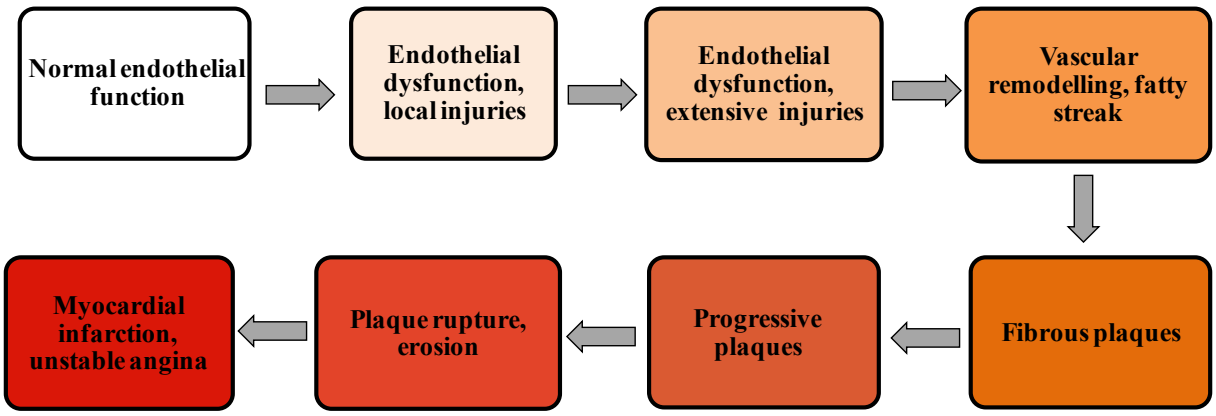

Figure 6: Atherosclerosis and endothelial dysfunction. The graph is reproduced from the article of A. Vértes.[21]

2.2 Technical background

2.2.1 Imaging techniques of the coronary arteries

Studies suggest that endothelial dysfunction is an early marker of CAD and can be detected before any structural changes to the vessel wall become apparent on conventional x-ray angiography or ultrasound. Therefore, by assessing the coronary endothelial function, it is thus possible to detect early manifestation of CAD and monitor their progression or regression.
Different imaging techniques are available to assess atherosclerotic coronary artery. Some of them are invasive (e.g., x-ray angiography, intravascular ultrasound, ultrafast computed tomography and angioscopy), while others are non-invasive (surface B-mode ultrasound and magnetic resonance imaging).[22]
Conventional x-ray angiography can only assess the luminal vessel diameter and, therefore, it underestimates the true burden of atherosclerosis, since it does not provide any information on coronary vessel wall thickness and the formation of atherosclerotic plaques. On the other hand intravascular ultrasound techniques allow imaging of the coronary plaques and assessing the lesion-site cross-sectional area and minimum lesion diameter, which are good predictors for CAD. However, intravascular ultrasound is an invasive technique, which is an important limitation. [8, 23]

2.2.2 Magnetic Resonance Imaging for coronary artery assessment

Unlike x-ray angiography and intravascular ultrasound, MRI is a non-invasive imaging modality with excellent soft-tissue contrast capable of visualizing the vessel wall and vessel lumen of the coronaries. Recent studies have demonstrated that MRI could not only identify morphological features of atherosclerotic plaques, but also characterize their composition in terms of lipid and fibrous content.[22] However, imaging coronary arteries with MRI remains challenging for several reasons [24]:

- small diameter (3-4 mm) and wall thickness (< 0.5 mm) of the vessels
- tortuous pathway
- their proximity to epicardial fat and myocardium
- the cardiac and respiratory motion

In addition, MRI still has some limitations to address: it is not a possible imaging technique for patients that suffer from claustrophobia and that have non-MR compatible implants, and the scan time efficiency is still too low. However the advantages introduced by the advent of MRI are remarkable.
To better understand how coronary artery can be assessed with MRI, the following section briefly introduces the main concepts of this technique. This section also describes techniques to address both cardiac and respiratory motions. For further details about MRI, the reader is referred to Haacke et al. [25].

Figure 7: 3T scanner Magnetom Prisma, Siemens Healthcare.

Overview of MRI

The main components of a MR system are: a magnet to generate a strong static magnetic field, a shim coil to make the magnet homogenous, a radiofrequency (RF) coil to transmit a radio signal to the imaged object, a receiver coil to detect the return radio signals, gradient coils to modulate the signal and a computer to reconstruct the radio signals into the final image.
The MRI signal is generated by the hydrogen atoms, which makes up the 60% of the human body. The strong static magnetic field $\mathbf{B_0}$ inside the MR room causes the protons of the hydrogen atoms to align parallel with $\mathbf{B_0}$ and to precess at the Larmor frequency $\boldsymbol{\omega_o}$ (Figure 8a)

$$\boldsymbol{\omega_o = \gamma B_o}, \tag{2.1}$$

where $\boldsymbol{\gamma}$ is a physical constant called gyromagnetic ratio.
The charges of each nuclei in combination with their precession motion produce a microscopic magnetic field $\boldsymbol{\mu = \gamma J}$. The sum of the microscopic magnetic fields from all the nuclei constitutes the source of the MR signal, the magnetization $\mathbf{M_z}$.
By applying an external magnetic field $\mathbf{B}$, the magnetization $\mathbf{M_z}$ rotates from its equilibrium position, *i.e.* along the direction of the applied magnetic field $\mathbf{B_0}$, to the transverse plane (x-y plane), yielding a transverse magnetization $\mathbf{M_{xy}}$. The time constant that describes how the longitudinal magnetization returns to the equilibrium position is called the spin-lattice relaxation time T_1 (Figure 8c). When the RF pulse is turned off, the magnetization in the transverse plane is dephased and comes back to its initial equilibrium position. The time constant that describes how the transverse magnetization $\mathbf{M_{xy}}$ returns to its equilibrium position is called spin-spin relaxation time T_2 (Figure 8d).

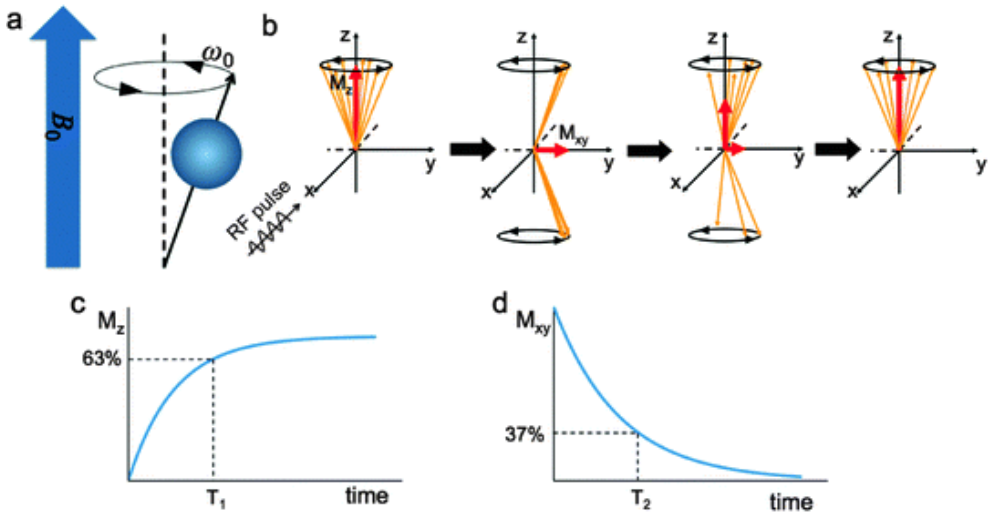

Figure 8: Precession at Larmor frequency of the spin of the hydrogen atoms due to the application of the static magnetic field B_0 (a). The application of the RF pulse makes the longitudinal magnetization M_z rotates to the transverse plane (transverse magnetization M_{xy}). By turning off the RF pulse, the longitudinal magnetization returns to its equilibrium position along the direction of the applied magnetic field B_0 (b). The recovery of the longitudinal and transverse magnetizations is described by the spin-lattice (c) and spin-spin relaxation time (d). [26]

The interaction between the magnetization and the external magnetic field **B** is described by the Block equation [44], from which it is then possible to derive the MR signal equation:

$$s(t) = \int_R m(\mathbf{r}) e^{-i\gamma \mathbf{r} \cdot \int_0^t \mathbf{G}(\tau) d\tau} d\mathbf{r} \tag{2.2}$$

By defining

$$\mathbf{k}(t) := \frac{\gamma}{2\pi} \int_0^t \mathbf{G}(\tau) d\tau \tag{2.3}$$

and substituting k(t) in the equation 2.2, it is evident that the MR signal equation is a Fourier transform operation

$$s\big(\mathbf{k}(t)\big) = \int_R m(\mathbf{r}) e^{-i2\pi \mathbf{r} \cdot \mathbf{k}} d\mathbf{r} \tag{2.4}$$

Therefore, the initial image can simply be reconstructed by computing the inverse Fourier transform,

$$m(\mathbf{r}) = \int_{\mathbf{K}} s(\mathbf{k}) e^{+i2\pi \mathbf{r} \cdot \mathbf{k}} d\mathbf{k} \tag{2.5}$$

Equation [insert number k(t)] describes that the gradient, $\mathbf{G}(t)$, controls the k-space trajectory, $\mathbf{k}(t)$. In other words, the magnetization is spatially encoded by changing the local magnetic field. The spatial encoding needs three different gradients, $\mathbf{G_x}$ $\mathbf{G_y}$ $\mathbf{G_z}$, since a magnetic field gradient is a variation of the magnetic field with respect to position. The application of these gradients modifies the direction of the magnetic field with respect to the main longitudinal $\mathbf{B_0}$ field.

The data acquisitions are mapped into a k-space, which is traversed line-by line. By changing the amplitude of the gradients, it is possible to modify the trajectories with which the k-space is traversed, and thus fully cover the k-space (Figure 9).

The k-space can be traversed using a Cartesian trajectory, as shown in Figure 9, or it can be traversed using non-Cartesian trajectories, such as radial or spiral trajectories.

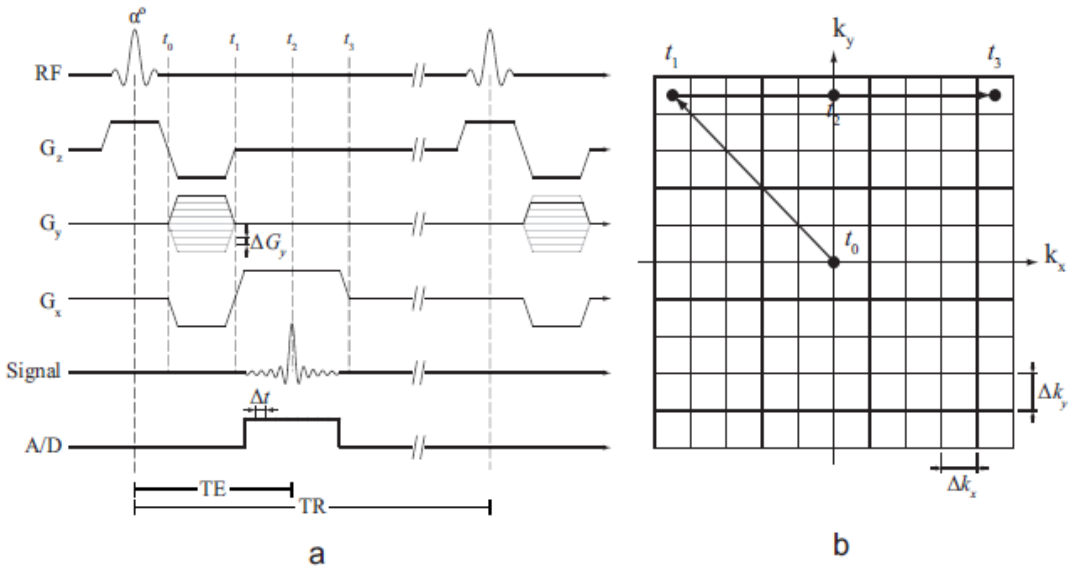

Figure 9: Gradient-recalled echo pulse sequence for a Cartesian 2D acquisition (a) and its corresponding k-space trajectories (b).

MRI is a very versatile imaging modality that can provide structural and functional information as well as different imaging contrasts. The main imaging parameters of MRI are the flip angle, the repetition time (TR), *i.e.* the time between two successive RF pulses to create transverse magnetization, and the time at which the signal is measured (TE). An alteration of these parameters generates images with a specific and different type of soft-tissue contrast (T_1 weighted, T_2 weighted, proton density weighted).[27]

Cardiac Motion: Retrospectively Gated Cardiac Cine Imaging

Image acquisition in MRI is intrinsically slow and is, therefore, susceptible to motion artifacts. If not corrected for, the periodic motion of the heart caused by cardiac pulsation can result in image blurring and degradation, such as ghosting artifacts. It is, therefore, fundamental to correct for

this motion, by synchronizing or gating the acquisition with the electrocardiogram (ECG) signal. Figure 10 illustrates an example of retrospectively gated cardiac cine imaging. The image acquisition is constantly gated with the ECG signal and starts always at the same phase of the cardiac cycle that usually corresponds to the QRS complex or R wave of the ECG. The image acquisition is performed over several cardiac cycles for a length of time equal to the maximum expected cardiac cycle length, *i.e.* R-R interval. Generally, the R wave is used to synchronize the data acquisition with the cardiac cycle, because it has the highest amplitude peak and sharpest upstroke. A small set of phase encoding steps are repeated within a cardiac cycle, and with each R wave, the phase encoding gradients are changed to acquire the next set of phase encoding steps (Figure 10). The process is repeated until all steps necessary for the image formation are collected. By using the temporal information about when data sampling occurred with respect to the R wave, the readouts are grouped into their corresponding cardiac phase. Finally, the images corresponding to each cardiac phase are reconstructed to create cine images that characterize the cardiac motion.[28]

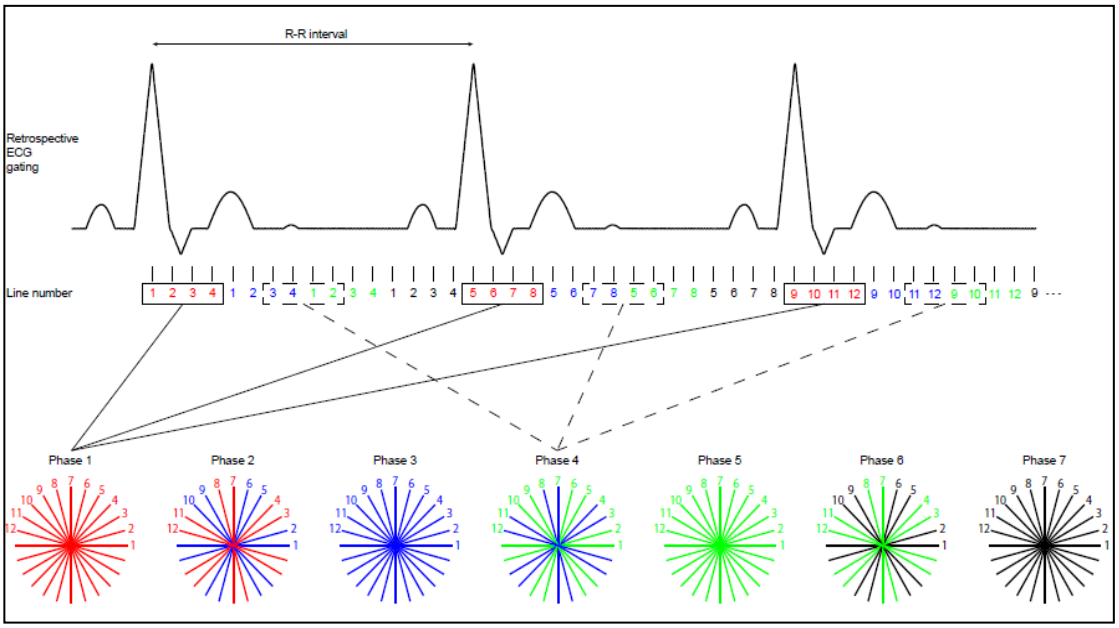

Figure 10: Retrospective ECG gating technique.

Respiratory Motion: Breathholding

In addition to the periodic motion of the heart, cardiac imaging also requires to deal with the respiratory motion. Different techniques are available to compensate for the respirator motion, such as by averaging acquisitions over multiple respiratory cycles or by ordering the phase encoding steps by respiratory phase, for example by acquiring the peripheries of the k-space during inspiration and the central part during expiration. Another possible approach is to ask the patient to hold his breath during data acquisition. This method helps reducing the artefacts

caused by the respiratory motion, but it is limited to short acquisition time since patients cannot hold their breath for more than 12-18 heart beats.[28]

Imaging of Coronary Artery: Bright-Blood Technique

Different acquisition schemes have been used in order to assess the coronary artery and its morphological features, such as bright-blood and dark-blood techniques.
Dark-blood techniques allow better visualizing the vessel wall and atherosclerotic plaques by using a double inversion pulse to suppress blood signal.[29] On the other hand, bright-blood technique permits to better visualize the lumen of the coronary artery. Such technique can be used to measure the cross-sectional area of the coronary artery and consequently measure its vasomotor response. The goal of this thesis is to assess coronary endothelial function by evaluating the vasodilatation of the coronary artery with a bright-blood imaging technique.
Bright-blood techniques use the *Time-of-flight* (TOF) effect to create images with bright blood contrast by manipulating the magnitude of the magnetization. It is a gradient echo technique that uses relatively short TR in order to saturate the static tissues and enhance the inflow of unsaturated flowing blood in the imaged slice.[30]
A small TR saturates the longitudinal magnetization M_z of the spins by preventing full recovery of the magnetization between each repetition of RF pulses. After several consecutive RF pulses, the longitudinal magnetization reaches a steady state and becomes saturated. This means that the amplitude and the intensity of the signal from the static tissues will be diminished.
On the other hand, blood from outside the imaged slice has not seen any RF pulse, so when the flowing blood spins enter the slice, they have unsaturated, full longitudinal magnetization. As a result, the intensity of the signal from the inflowing spins is greater than the signal from the static spins that have experienced multiple RF pulses, and this contrast makes the blood signal to appear bright in the gradient-echo images (Figure 11a-b).[31]

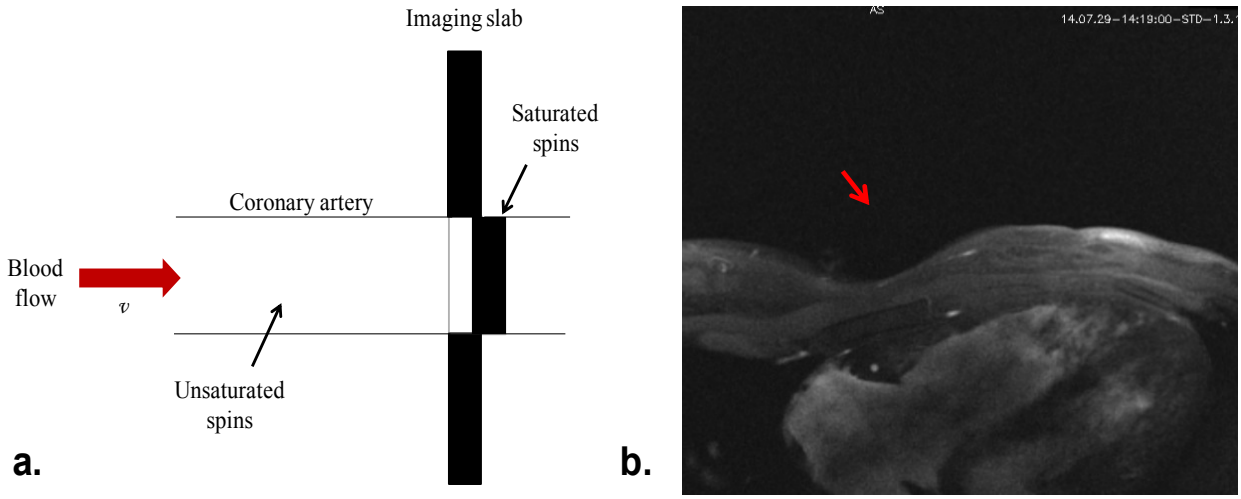

Figure 11: a.) After multiple receiver pulses RF, the longitudinal magnetization cannot anymore fully recover and it becomes saturated. The flowing blood has not experienced any RF pulses and enters inside the imaging slab with fully magnetization, generating a bright signal compared to the one of the soft tissues outside the vessel that look dark. b.) Cross-section of the right coronary artery (RCA) (red arrow) obtained using the bright-blood technique.

2.3 Compressed Sensing (CS) reconstruction

The breathhold duration limits the acquisition time and, in turns, the spatial and temporal resolutions of the cine images that is achievable in that amount of time. Therefore, the images obtained with the standard retrospective binning are often under-sampled. This means that for each image, there are fewer lines of the k-space acquired than what is prescribed by the Nyquist-Shannon sampling theorem. A reconstruction technique more advanced than the simple Fourier transform is then necessary to recover the initial image.

The k-space can be traversed by straight lines, using Cartesian sampling, with which the reconstruction is then obtained by simply applying the inverse Fast Fourier Transform. Other possible non-Cartesian trajectories are now in use, such as sampling along radial lines. A non-Cartesian sampling is able to take into account the energy distribution of MR images in k-space, by over-sampling the center, which has high energy, and under-sample the periphery. (Figure 12)

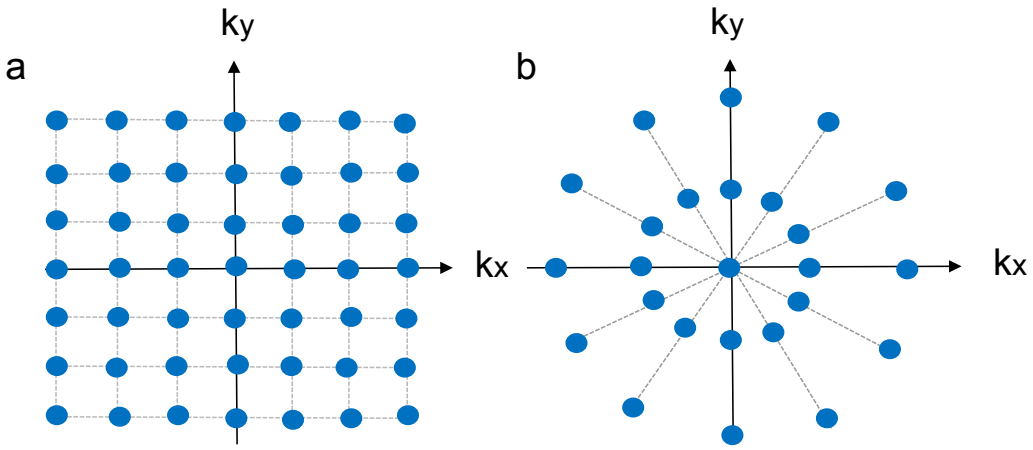

Figure 12: 2D representation of Cartesian (a) and radial (b) acquisition.

In general the k-space is traversed slowly because of physiological and physical limitations. Physical limitations concern the maximum amplitude and slew-rate that the gradients can achieve. At the same time, the high amplitude of the gradients and the rapid switching of the magnetic fields can induce electric fields in the patients that can cause nerve stimulation. It is then necessary to find an alternating way to speed up the acquisition time, which is nowadays one of the main challenging tasks in MRI. It could bring an improvement in patient care and a reduction of health care costs.

The main idea of Compressed Sensing (CS) is to reduce the number of data acquired without affecting the quality of the images, and consequently to speed up the image acquisition during a MR exam.

CS builds upon the fact that most of the signals are sparse in some domains. In general a vector is *k*-sparse if it has at most *k* non-zeros coefficients. Most images are not directly sparse, but they admit a sparse representation in some special basis $\boldsymbol{\psi}$**.** Mathematically speaking, the sparsifying transform is an orthonormal basis $\boldsymbol{\psi}$ that defines the sparse representation $\mathbf{w}=\boldsymbol{\psi}\mathbf{m}$ of an image **m**. Medical images are an example of images that can be compressed using an appropriate sparsifying transform (Figure 13).

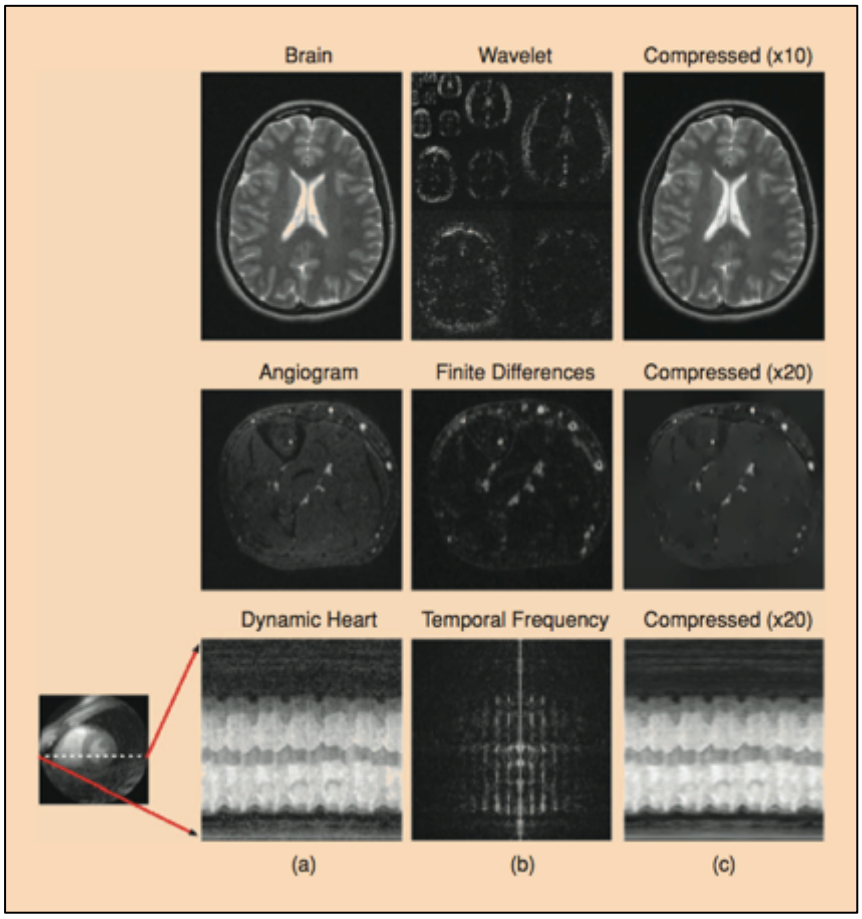

Figure 13: Transform sparsity of MR images. (a) Fully sampled images are mapped by a sparifying transform to a (b) transform domain. The largest coefficients are maintained while the others are set to zero. The transform is then inverted and the reconstructed image (c) is formed.[40]

The second principle on which CS relies is the incoherence between the sampling and the sparse domain. The aliasing artefacts are generated by a violation of the Nyquist –Shannon sampling theorem (see the Parallel-imaging section). These artefacts can be coherent when the undersampling are equally spaced, incoherent when the sampling is irregular. The aliasing artefacts in a linear reconstruction caused by k-space undersampling must be incoherent (noise-like) in the sparsifying transform domain. These key concepts of CS are illustrated in Figure 14. The signal (Figure 14 (1)) is sparse meaning that it has only a few nonzero values. Figure 14 (2) illustrates the Fourier transform of the signal in Figure 14 (1). Uniform undersampling of the Fourier coefficients leads to coherent aliasing artifacts (Figure 14 (4), whereas random undersampling leads to incoherent or noise-like aliasing artifacts. The zero-filled Fourier reconstruction (Figure 14 (4)) looks like a noisy version of the signal. The largest nonzero values stand out above the level of interference, while the smallest one remains covered. By selecting a threshold it is possible to first detect and recover the highest values. The interference associated with these highest coefficients is then calculated and subtracted from the aliased signal, thus

lowering the total interference level and enabling the recovery of weaker coefficients. Finally, the process is repeated until all the components are recovered.[40]

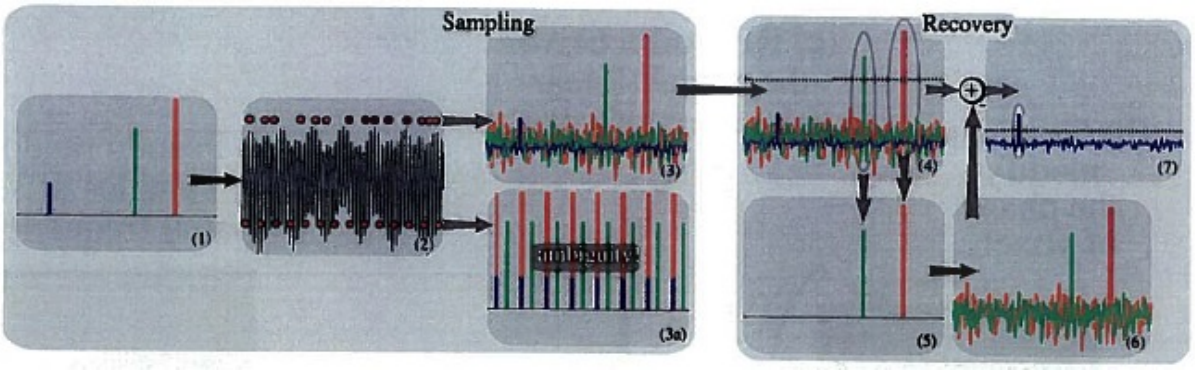

Figure 14: Intuitive Procedure for Reconstruction from Undersampled Data. A sparse signal (1) is 8-fold undersampled in its 1D k-space domain (2). Equispaced undersampling results in signal aliasing (3a) that cannot be recovered. Pseudo-random undersampling results in incoherent interference (3). Some strong signal components stick above the interference level, are detected and recovered by thresholding (4 and 5). The interference of these components is computed (6= and subtracted (7), thus lowering the total interference level and enabling recovery of weaker components.[40]

The above example described a simple iterative reconstruction that illustrates the key concepts of CS. However, in practice, CS reconstruction uses more advanced algorithms based on mathematical optimization. Images are reconstructed using a non-linear method where both sparsity of the image representation and consistency of the reconstruction are enforced. With a specific non-linear reconstruction, the noise-like artefacts can be suppressed without degrading the image quality.

CS is a mathematical framework for acquiring and reconstructing the images that can be represented as vectors $\mathbf{m} \in \mathbb{C}^n$. The image of interest is *a priori* compressible in a known base $\boldsymbol{\psi}$. If the observations are exact, i.e. no additive noise, the recovery of the signal is achieved by solving the constrained optimization problem:

$$\begin{aligned} &\text{minimize } ||\boldsymbol{\psi}\mathbf{m}||_1 \\ &\text{subject to } \mathbf{F_u m} = \mathbf{s}, \end{aligned} \tag{2.6}$$

where $\mathbf{F_u}$ is the undersampled Fourier transform and $\mathbf{s}$ is the signal containing the undersampled k-space data from the MRI scanner. In reality, the MR images are corrupted with noise, thus the problem to solve becomes:

$$\begin{aligned} &\text{minimize } ||\boldsymbol{\psi}\mathbf{m}||_1 \\ &\text{subject to } ||\mathbf{F_u}\,\mathbf{m} - \mathbf{s}||_2^2 \leq \boldsymbol{\epsilon}, \end{aligned} \tag{2.7}$$

where $\boldsymbol{\epsilon}$ controls the fidelity of the reconstruction to the measured data. Thus the first equation promotes the sparsity, while the second one enforces the data consistency. The above constrained problem can be reformulated as an unconstrained problem using the Lagrange formulation:

$$\text{argmin}_{\mathbf{m}} \, ||\mathbf{F_u m} - \mathbf{s}||_2^2 + \lambda \, ||\boldsymbol{\psi}\mathbf{m}||_1, \tag{2.8}$$

where λ is a regularization parameter, which weights the reconstruction between ensuring data consistency and enforcing sparsity.
All the observations presented are valid if there is only a single receiver-coil with uniform detection sensitivity. In reality, multichannel receiver array are often used. Generally the coil sensitivity describes how sensitive a given channel is to a specific point in space, and it is often dependent on the object in the receiver coil. The following section describes how multichannel receiver array are used in parallel imaging.

2.3.1 Parallel imaging and SENSE algorithm

Parallel Imaging is a reconstruction technique which requires a multichannel receiver array, and that can be used to reconstruct under-sampled data from any type of pulse sequence. There are different possible parallel imaging algorithms, such as SENSE and GRAPPA, both of them with the aim to reconstruct artefact-free images from the aliased ones. In fact, by undersampling the data, aliasing is introduced if the Nyquist criterion is not met.[41] More specifically, the Nyquist criterion says that the highest frequency signal that can be accurately digitized at a certain sampling frequency f_s is equal to half of the sampling frequency, known as Nyquist frequency f_N:[27]

$$f_N \geq 2f_s. \tag{2.9}$$

When a multichannel receiver array is used, it is necessary to combine in a single image all the images resulting from the multiple channels. There are different methods to combine the coil images and produce a final composite image. The sum-of-square method is the simplest one. The voxel of the composite image at the position **r,** m(**r**), is obtained by calculating the square root of the sum of the squared pixel values from each coil at position **r**:

$$m(\boldsymbol{r}) = \sqrt{m^*(\boldsymbol{r})\Lambda^{-1}m(\boldsymbol{r})} \tag{2.10}$$

where Λ is the noise covariance matrix.
Another method to combine the coil images into a single image is to use the spatial sensitivity information. An estimate of the spatial sensitivities can be obtained by dividing each coil image

by the sum-of-squares combined image. This spatial sensitivity information can then be used to accelerate MRI with parallel imaging.

SENSE is one of the standard reconstruction method for parallel imaging used in clinical settings. The only major drawback to SENSE reconstruction is the need of an accurate coil sensitivity map, which can be difficult to obtain. The image voxels are weighted with the coil sensitivity at the corresponding location in the full field of view (FOV). The SENSE reconstruction consists then in solving the set of linear equations:

$$\mathbf{m}' = \mathbf{C}\mathbf{m} \tag{2.11}$$

where $\mathbf{m}'$ is the concatenation of the aliased images from the coils, $\mathbf{m}$ is the final composite image and $\mathbf{C}$ is the sensitivity matrix.

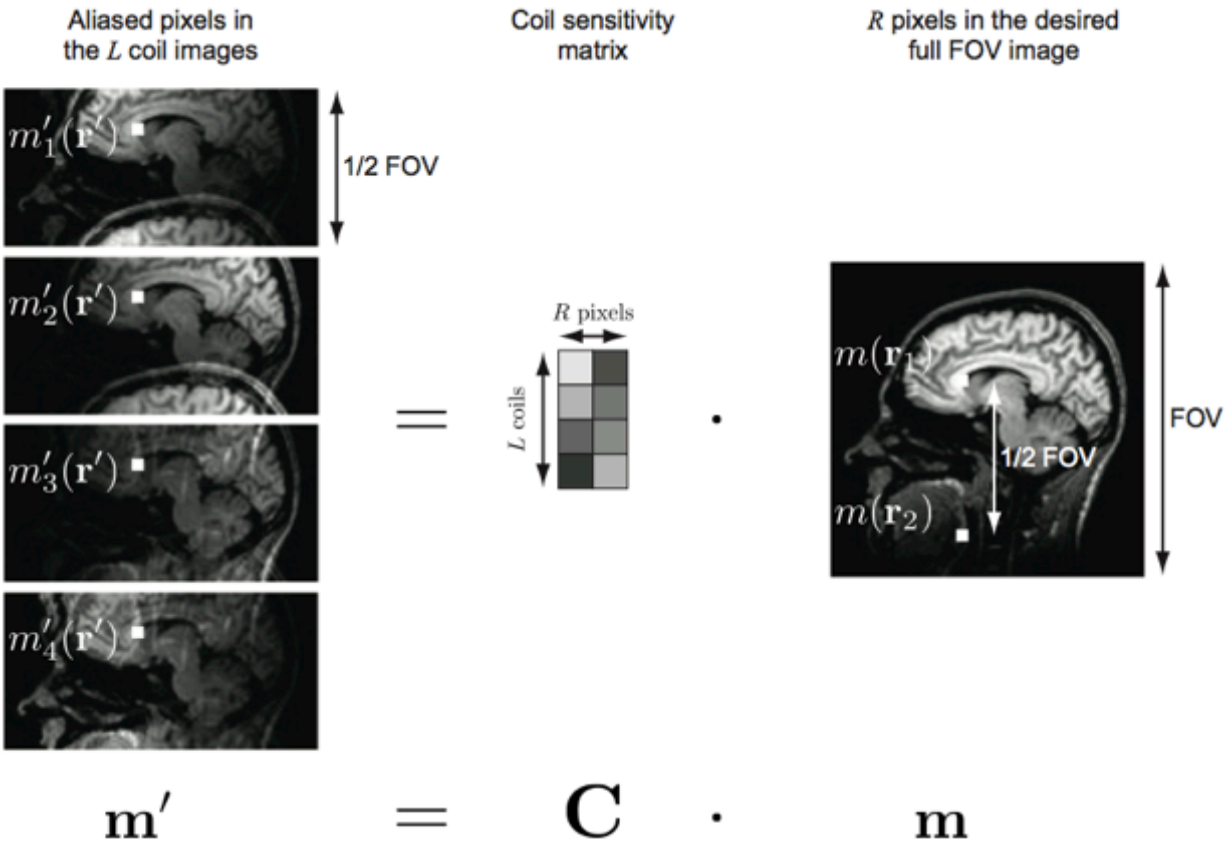

Figure 15: Illustration of SENSE reconstruction.

2.3.2 Sparse SENSE algorithm

Sparse SENSE is a combination between CS and SENSE. The reconstructed image is obtained by solving the following optimization problem:

$$\text{argmin}_{\mathbf{m}} \left|\left|\mathbf{Em} - \mathbf{s}\right|\right|_{\mathbf{2}}^{\mathbf{2}} + \lambda \left|\left|\boldsymbol{\psi}\mathbf{m}\right|\right|_{1}. \quad (2.12)$$

This problem is similar to the one that has to be solved in Compressed Sensing, but in this specific case **m** is the unknown final image, **s** is the vector obtained by concatenating the k-space data from all the coils and $\mathbf{E} = \mathbf{F_u C}$ is the sensitivity encoding matrix, which includes the undersampled Fourier transform and the coil sensitivity matrix. [41]

2.4 Assessment of endothelial function

A direct and non-invasive assessment of the vasomotor response could provide important information about CAD and its progression on patient, and an earlier diagnosis could initiate preventive treatments to reduce risks of myocardial infarctions.
Together with MRI, an endothelial dependent or independent vasomotor needs to be used in order to assess the vasomotor response. Endothelial dependent vasomotor causes a dilatation of the endothelium directly acting on the endothelium, while the endothelial independent vasomotor causes a dilatation of the endothelium as a consequence of other effects.
In previous studies the endothelium-dependent coronary vasodilatation using nitroglycerin (NTG) had been assessed, showing a clear correlation between impaired NTG-induced coronary vasodilatation and advanced formation of coronary artery calcification.[32]
MRI can also be combined with an endothelial-dependent vasomotor, such as an isometric handgrip exercise, in order to stress, dilate and non-invasively image the coronary arteries. An exercise test is in fact a useful method to obtain reliable information regarding CAD in patients.[33] By squeezing the handgrip, in healthy subjects the heart rate increases, as well as the blood flow and the blood pressure, and as consequence the coronary arteries dilate.
Previously, stress tests have already been combined with MRI, since they are an effective method to evaluate normal and abnormal cardiovascular function. A bicycle exercise within the scanner has been used, but the motion of the subject considerably affected the final image measurements.[34] By performing the bicycle exercise outside the MR room, these problems are avoided, but in the time elapsed from the exercise and the image acquisition, the subject's cardiovascular system could have been recovered.[35] The isometric handgrip exercise is thus a possible alternative, which allows performing a stress exercise within the scanner and avoiding motion artefacts.[36] In recent studies for endothelial function assessment an analog ergometer

has been used, which consists of an aluminum plate to display the grip strength to the volunteer (Figure 16).[10-12]

Figure 16: Analog handgrip device

This ergometer, however, has several drawbacks:

- A moving conductor in the magnetic field of the MR room, as the aluminum plate of the ergometer, experiences significant resistance due to eddy currents, which form around the device. Consequently the volunteer feels the device vibrating and these vibrations could affect the final success of the exercise.
- Because of these vibrations, the volunteer has to lie prone holding the ergometer outside the scanner, in order to reduce as much as possible the effect of eddy currents.
- In prone position, the volunteer cannot see the panel on which his grip strength is displayed, so the presence of a nurse inside the scanner room is necessary.

To address these limitations, the work in this thesis presents a new setup that substitutes the analog ergometer with a digital MR-compatible handgrip, which is not affected by eddy currents and allows a supine position for the volunteer. The digital ergometer does not have a panel to display the grip strength, thus it has to be integrated with a visual feedback system for the patient and the data need to be digitally recorded as a function of time during the MRI scanning.

2.5 Previous results

Previous studies have been conducted on the evaluation of the coronary endothelial response, in order to understand any possible correlations between CAD and endothelial functionality. These studies have demonstrated that MRI with an isometric analog handgrip exercise can be used to non-invasively and quantitatively evaluate the vasomotor response.[37, 38] The protocol used for the isometric handgrip exercise consisted of a few minutes handgrip exercise at 30% of the volunteer's maximum grip strength. In the work of Hays et al. [10], a different vasodilatation was clearly visible between the group of healthy and non healthy patients. The non healthy patients had an abnormal coronary endothelial response with a lack of vasodilatation and decreased flow. The images were acquired using clinical 3.0T MRI scanner, and through the cross-sectional area and flow velocity of the coronary artery were assessed (Figure 17-18). The cross sectional area was then manually traced and measured by a specific computer algorithm.[10]

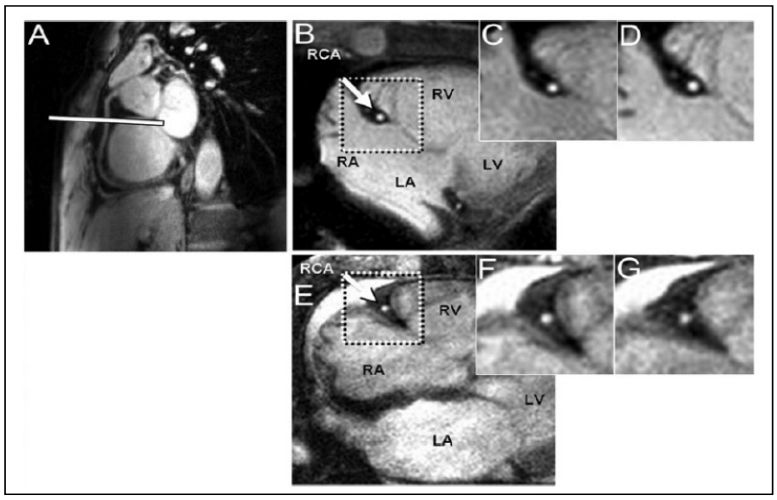

Figure 17: Typical anatomical coronary images using MRI at rest (image C and F) and with sequential handgrip stresses (image D and G) in a healthy subject (image B,C,D) and CAD patient (image E,F,G). Image A shows the scout scan with the location of the cross-sectional imaging plane placed perpendicular to the right coronary artery (white line). Image from reference [10]

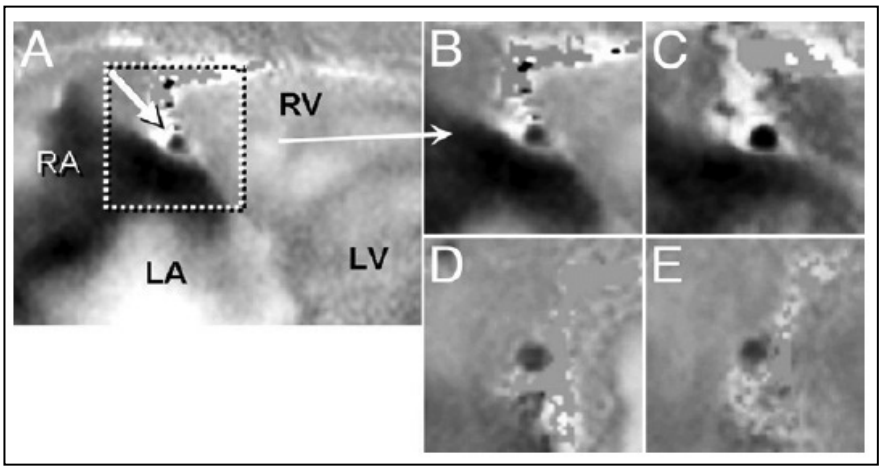

Figure 18: Flow Velocity-Encoded MRI Phase images. The black colour indicates the high velocity down through the image plane. Images B and C correspond to the flow in a healthy subject before and after isometric exercise, while images D and E show the flow before and after isometric exercise in a CAD patient. Image from reference [10]

Their results showed an increase of vasodilatation and blood flow of the coronary artery in healthy subjects as a response to isometric handgrip exercise, and a decrease in CAD patients. Handgrip exercise increased area by around 18% in healthy subjects and decreased it by around 6% in CAD patients.[10]

Thus it has been demonstrated that in the healthy subjects there is, after an isometric handgrip exercise, an increase in cross-sectional area and blood flow, while in CAD patients there is a decrease in all these features.

Healthy subject	CAD subject
↑ Vasodilatation	↓ Vasodilatation
↑ Cross-sectional area	↓ Cross-sectional area
↑ Blood flow	↓ Blood flow

To confirm that the vasoconstriction of the coronary artery observed in CAD patients depends only on the abnormal endothelial function and not on other causes, they administrated nitroglycerin, an independent vasodilator, and observed that the coronary artery dilates in the same way both in healthy and CAD patients (Figure 19).

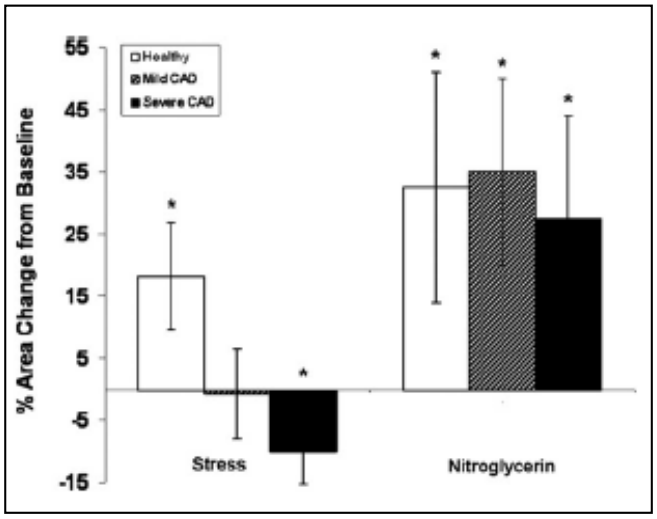

Figure 19: Endothelial-dependent and -independent vasoreactivity in healthy volunteers (white bar), patients with mild CAD (gray bar) and patients with severe CAD (black bar) patients. Image from reference [10]

One of the early manifestations of atherosclerosis is an increased coronary wall thickness. In order to better quantify the vessel wall thickness and the luminal area, black blood MRI sequences have been used (Figure 20) [11]. These sequences allow visualization of the vessel wall and non-invasive detection of subclinical coronary atherosclerosis.[11]

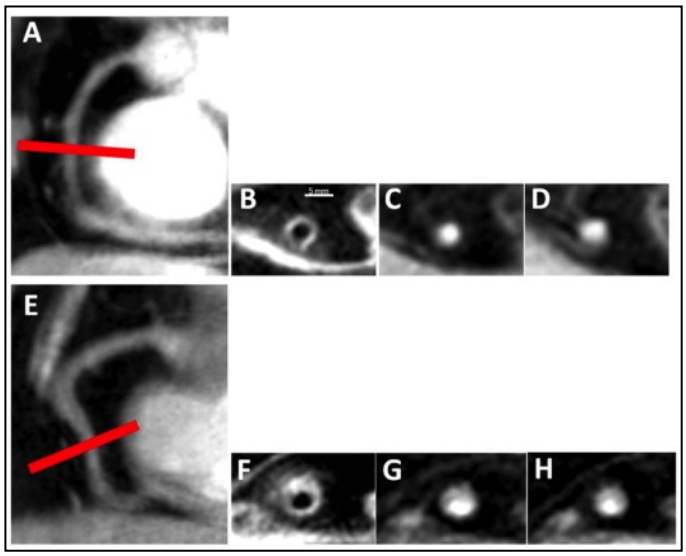

Figure 20: Images using MRI of a healthy subject (A-D) and of a CAD patient (E-H). Images C and G are acquired at rest, while images D and H are acquired during stress. Image from reference [11]

Figure 20, shows images acquired in a healthy volunteer (Figure 20A-D) and in a CAD patient (Figure 20E-H). The vessel wall of the CAD patient (Figure 20F) has an irregular shape, due to the presence of atherosclerotic plaques, and it is thicker than the one of the healthy subject (Figure 20B).

The reliability of the measurements obtained by combining MRI with isometric handgrip exercise was also tested and validated by performing sequential isometric exercises both in CAD patients and healthy adults [12]. It was shown that the measures remained unchanged during repeated stress tests (Figure 21).

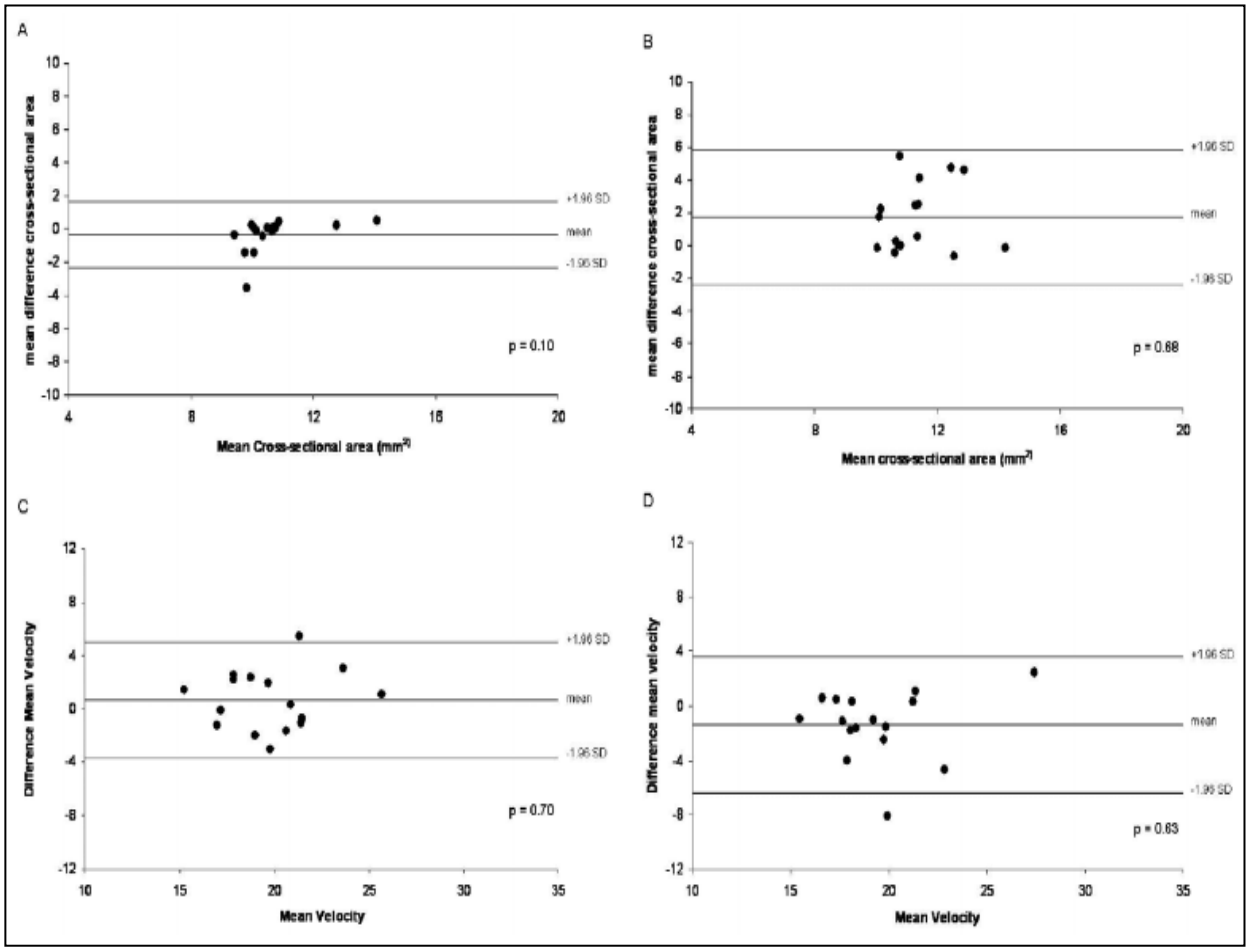

Figure 21: Bland-Altman plots for intra-observer and inter-observer variability. Bland-Altman plots for intra-observer variability (A and C) and inter-observer variability (B and D) of coronary artery cross-sectional area (A and B) and peak diastolic flow velocity (C and D) measurements in CAD patients and healthy subjects. Solid lines above and below the mean represent 2 standard deviations and the mean differences are shown. P-values are derived from Pitman's test of differences. Image from reference [12].

The results obtained so far demonstrate that this technique could be used in the future for a non-invasive assessment of the coronary artery and it could give important prognostic information in order to predict future cardiovascular events in patients.

3 Methods

This chapter presents all the methods that have been used and implemented in this work. The first section is about the MR compatible digital handgrip. It describes the general set-up for the isometric handgrip exercise, the handgrip linearity test, the protocol used for the isometric exercise and the techniques used as feedback. The second section is about the methods used for coronary endothelial function assessment: the techniques used for image acquisition and their comparison, the measurements of the cross-sectional area.

3.1 MR compatible digital handgrip

The coronary endothelial function can be studied and assessed by evaluating the vasodilatation of the endothelium in response to isometric handgrip exercise. The exercise is performed within the scanner, so the images of the coronary artery can be acquired before and after the isometric handgrip exercise.
The digital handgrip is held by the volunteer inside the scanning room and connected to a workstation outside the MR room through a fiber optic cable. An interface device, *fORP interface 932*, converts the optical signal from the handheld device into an electrical signals that is then transferred to a control workstation via a USB connection (Figure 22).[39]

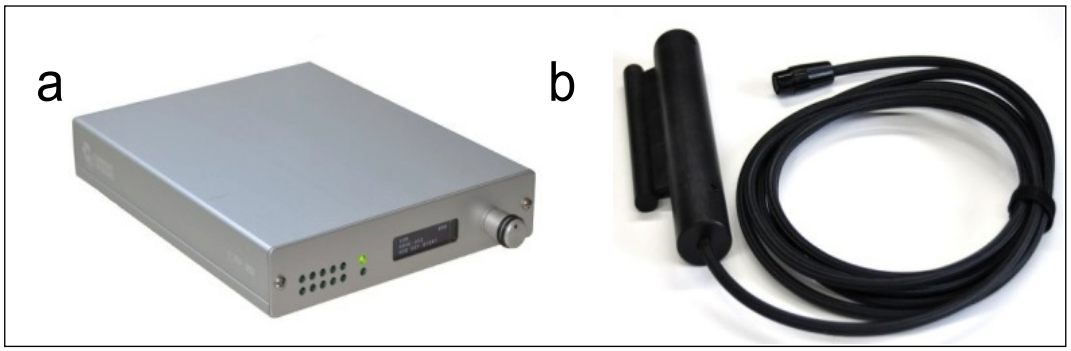

Figure 22: 32-Channel electronic Interface (a), which receives optical signals from the Grip Force Fiber Optic Response Pad (b).

The workstation continuously records the handgrip strength of the volunteer and collects the data in a text file for future processing.
Unlike the analog ergometer, the digital one does not have a panel on which the grip strength is displayed. It is therefore necessary to integrate the digital handgrip with a real-time visual feedback that shows the user's grip strength. A custom-written MATLAB (The MathWorks, Inc) program has been implemented to record and display the grip strength. A projector placed outside the MR room and connected to the workstation, displays the visual feedback on a screen placed at the back of the scanner.
A system of mirror is used to allow the volunteer to see the screen placed at the back of the scanner (Figure 23).

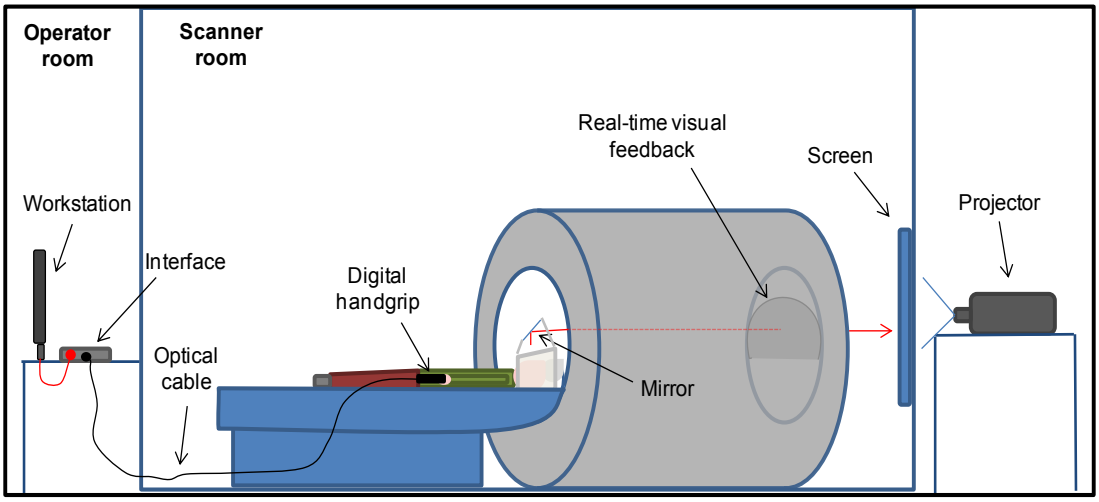

Figure 23: Schematic illustration of the set-up used for the isometric handgrip exercise: real-time visual feedback integrated with MRI.

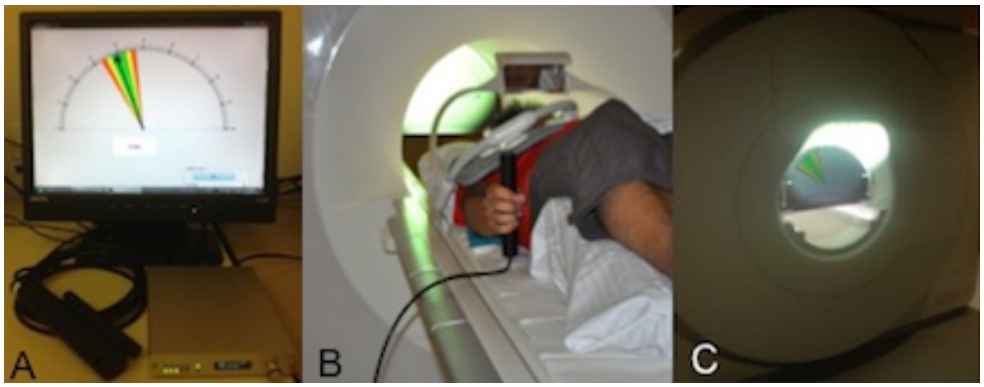

Figure 24: The main components of the implemented set-up. A) The interface is connected to the workstation via USB cable, placed outside the MR room. B) A panel is placed behind the scanner, on which a projector displays the real-time visual feedback. C) The volunteer is lying in a supine position and he is holding the handgrip device (solid arrow) with his dominant hand. The volunteer can directly see the screen placed behind the scanner through a system of mirrors (dashed arrow).

3.1.1 Handgrip linearity test

A test was designed to verify the linearity of the handgrip's response. The test consisted of applying increasing weights and measuring the handgrip response. A polynomial fit was used to verify the general behaviour of the ergometer. The set-up used to perform the test is shown in figure 25.

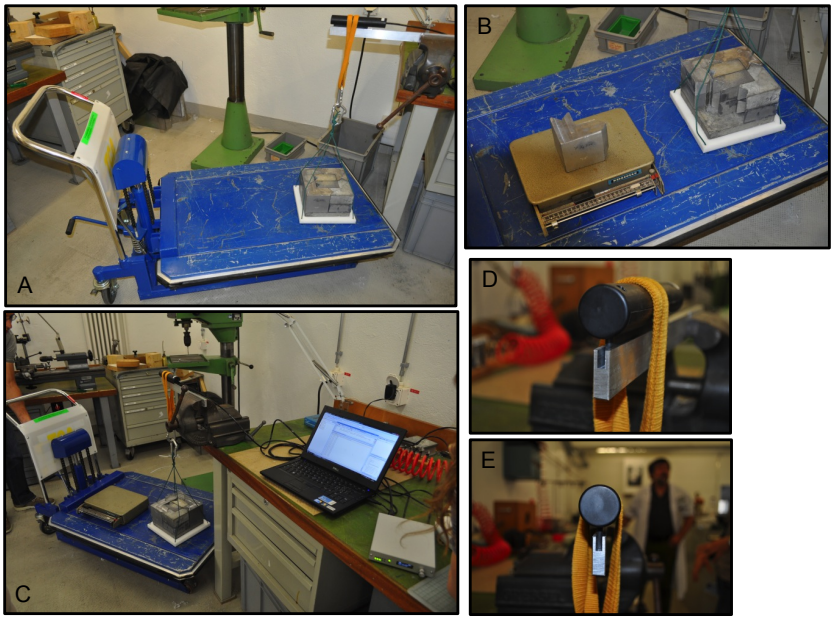

Figure 25: Set-up of the linearity test. General set-up for the experiment (Fig. A-B-C) and details of the handgrip with the rope on it (Fig D-E).

The handgrip was fixed on a metal bar, and a rope connected to a frame by a snap-hook was lead on the handgrip. The experiment consisted in increasing the weights applied on the frame starting from 0 kg and progressively reaching the maximum weight of 49.79 kg, since the maximum force applicable on the handgrip is about 500 N.
The response of the handgrip was constantly monitored by recording the grip strength values.
The experiment was performed twice, first starting with the maximum applicable weight on the handgrip and then reducing it, and the second time starting from 0 kg and then increasing the weight.

3.1.2 Handgrip technique and protocol

The volunteer holds the MR-compatible digital handgrip with his dominant hand while he/she is lying on the MR bed. The protocol of the isometric handgrip exercise is summarized in Figure 26. Prior to imaging, the volunteer is required to squeeze the handgrip as much as possible and the maximum grip strength is registered. The maximum force that can be applied to the digital handgrip is limited to 500N, which corresponds to a weight of about 51 kg. The visual feedback is then updated according to the maximum force of the volunteer.
Images of the coronary artery are acquired before and after the stress test in order to measure the changes in lumen area. The images are acquired at end expiration and the acquisition lasts about 20 seconds. Therefore, each acquisition is preceded by a breath in-breath out respiration cycle in order to prepare the volunteer for the 20 seconds breathhold. The breath-holding technique allows reducing the additional artefacts due to respiratory motion.
For the isometric handgrip exercise, the volunteer is asked to start squeezing the handgrip at 30% of his maximal force 30 seconds before the acquisition and to maintain his grip during the ~20 seconds data acquisition. The 30% is clearly indicated on the screen by a green coloured zone.

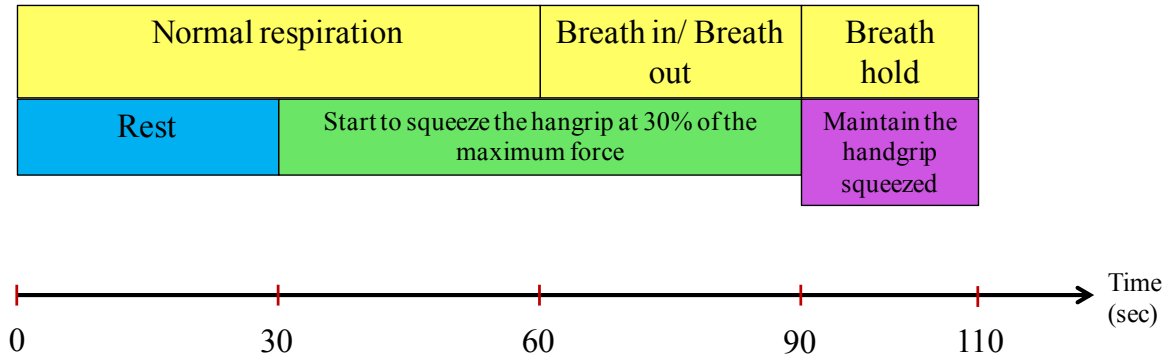

Figure 26: Protocol for the isometric handgrip exercise showing the time approximation for each step. During the first 30 seconds the volunteer rests and breaths normally. For the next 30 seconds, the volunteer starts to squeeze the handgrip at 30% of his maximal force while breathing normally. Next the volunteer is required to breath in-breath out twice before starting the acquisition. During the acquisition, the volunteer hold his breath at end expiration. The handgrip has to be maintained squeezed for the whole duration of the protocol.

3.1.3 Real-time visual feedback

The innovative feature of the implemented set-up for digital isometric handgrip exercise is the direct feedback of the force squeezed with the handgrip by looking on the real-time visual feedback.
The fORP interface is connected via a USB-converter to the workstation located in the operator room and the self-written MATLAB program reads the force applied to the handgrip. The real-

time visual feedback consists of a protractor style half-circle scale with values between 0 and 100. An arrow indicates the actual force applied to the handgrip by the volunteer. The isometric exercise consists of two phases: a self-calibrating phase called *First pass acquisition* and an acquisition phase called *Acquisition pass*. A popup menu in the panel allows selecting which part of the exercise is going to be performed (Figure 27). By choosing *First pass acquisition,* the volunteer has to squeeze as much as he can and the maximum force is recorded to calibrate the handgrip device. Then by selecting *Acquisition pass* from the popup menu, the second part of the exercise can be performed. During the second phase, the volunteer has to maintain the arrow in the green zone, which corresponds to the 30% of the volunteer's maximal force. A timer at the bottom of the display helps the volunteer to count 30 seconds, during which he has to maintain the handgrip squeezed. (Figure 28)

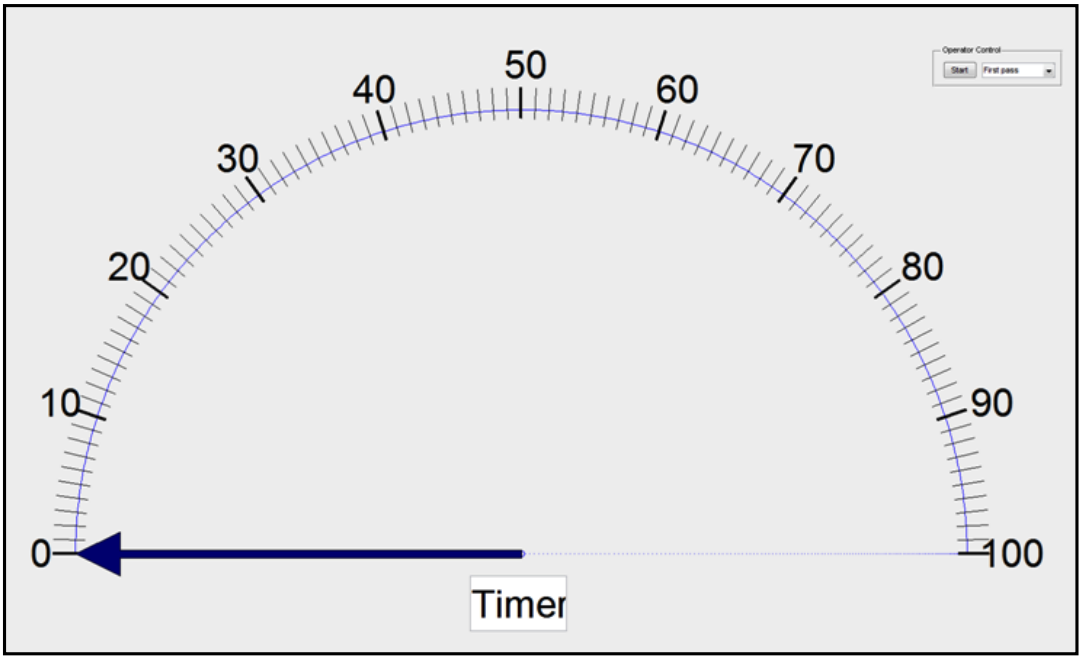

Figure 27: Real-time visual feedback. The blue arrow rotates in accordance to the squeezed grip strength of the volunteer. In the upper right corner of the screen, there is the operator control panel, which contains the start button and the popup menu.

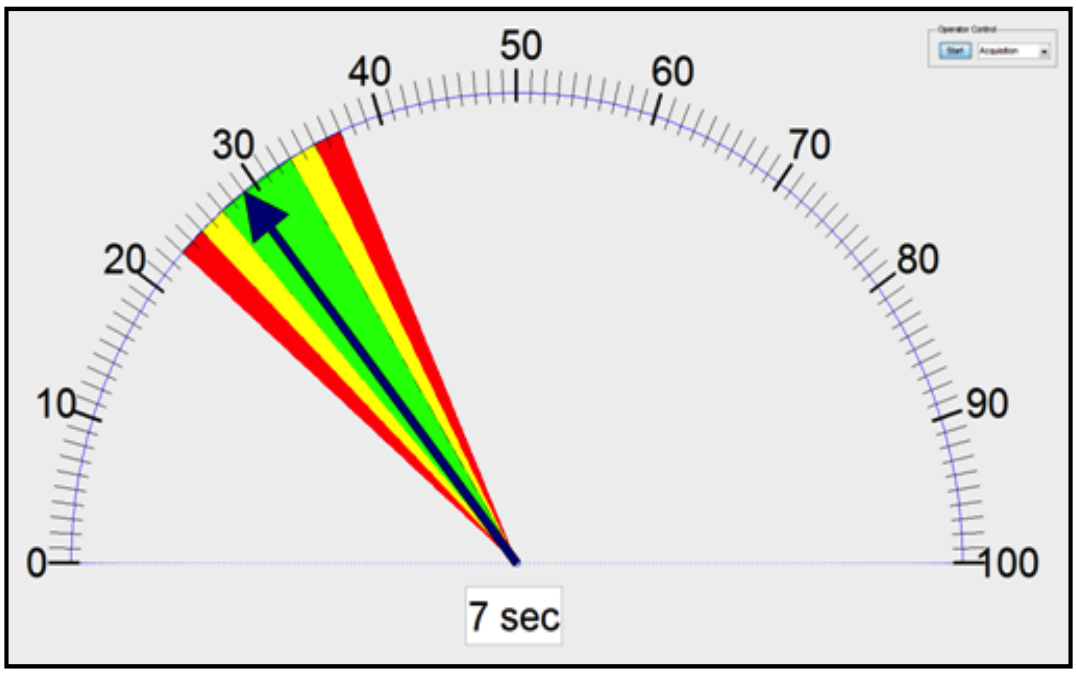

Figure 28: Real-time visual feedback. The green zone represents 30% of the maximal grip strength of the volunteer. At the bottom of the screen a timer shows the duration of the isometric handgrip exercise in second.

The data of the *First pass acquisition* and the *Acquisition pass* are collected in two different files so it is possible to plot them and see the general trend of the volunteer's strength during the isometric handgrip exercise.

3.1.4 Survey

At a later stage the analog handgrip has been tested as well on volunteers, following the same protocol than the one used with the digital handgrip. Compared to the digital one, the analog handgrip cannot provide any feedback to the operator about how the volunteer performs the exercise since the grip strength values are only displayed on the aluminium panel attached to the handgrip. It is thus necessary to provide the operator with a possible feedback. In order to achieve that, at the end of the scan all the volunteers filled up a survey previously prepared, which aims to evaluate the impressions of the volunteer while performing the exercise (Figure 29). All the questions included in the survey compare different aspects and features of the isometric handgrip exercise with both the analog and the digital device.

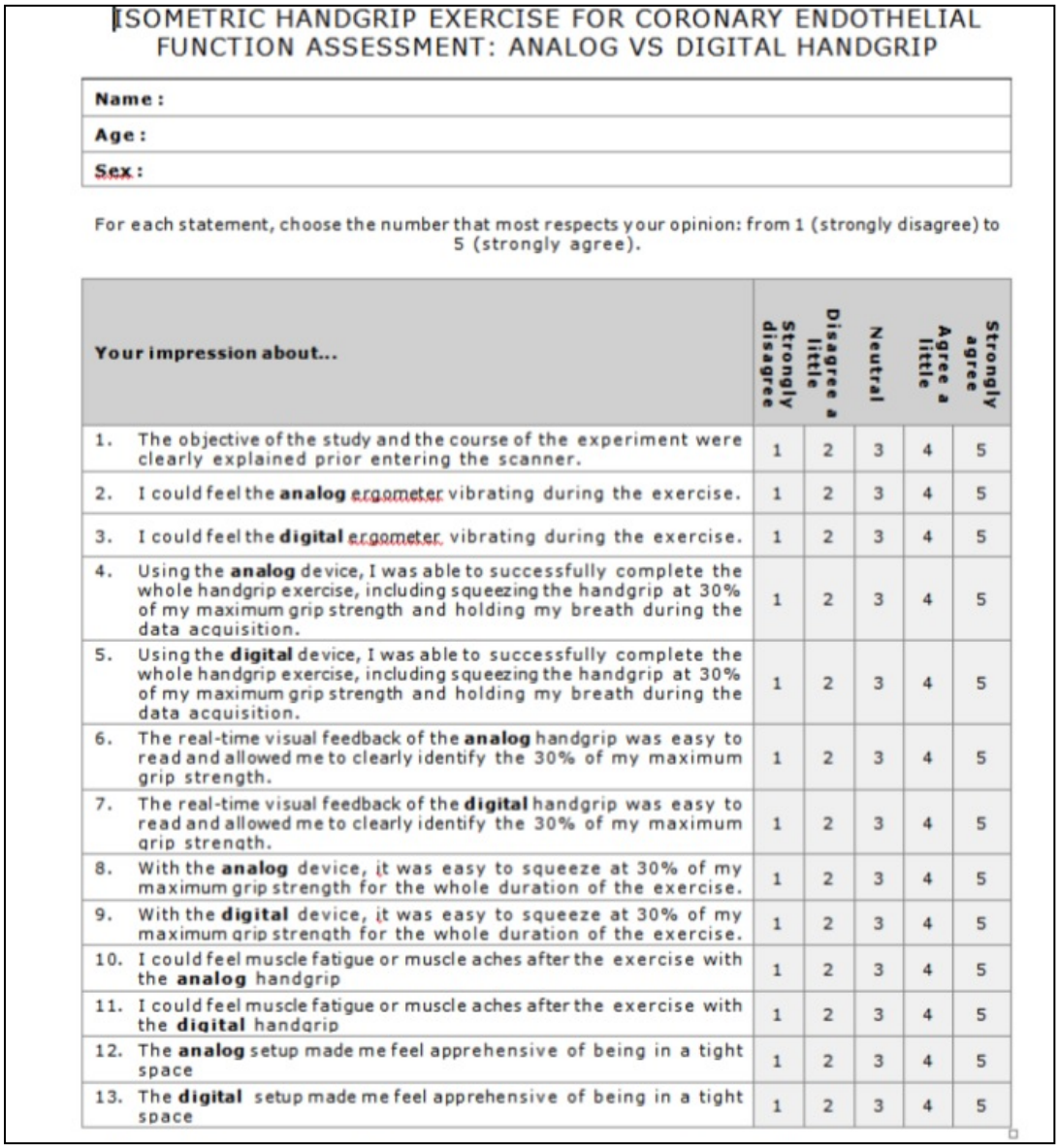

ISOMETRIC HANDGRIP EXERCISE FOR CORONARY ENDOTHELIAL FUNCTION ASSESSMENT: ANALOG VS DIGITAL HANDGRIP

Name :	
Age :	
Sex :	

For each statement, choose the number that most respects your opinion: from 1 (strongly disagree) to 5 (strongly agree).

Your impression about...	**Strongly disagree**	**Disagree a little**	**Neutral**	**Agree a little**	**Strongly agree**
1. The objective of the study and the course of the experiment were clearly explained prior entering the scanner.	1	2	3	4	5
2. I could feel the **analog** ergometer vibrating during the exercise.	1	2	3	4	5
3. I could feel the **digital** ergometer vibrating during the exercise.	1	2	3	4	5
4. Using the **analog** device, I was able to successfully complete the whole handgrip exercise, including squeezing the handgrip at 30% of my maximum grip strength and holding my breath during the data acquisition.	1	2	3	4	5
5. Using the **digital** device, I was able to successfully complete the whole handgrip exercise, including squeezing the handgrip at 30% of my maximum grip strength and holding my breath during the data acquisition.	1	2	3	4	5
6. The real-time visual feedback of the **analog** handgrip was easy to read and allowed me to clearly identify the 30% of my maximum grip strength.	1	2	3	4	5
7. The real-time visual feedback of the **digital** handgrip was easy to read and allowed me to clearly identify the 30% of my maximum grip strength.	1	2	3	4	5
8. With the **analog** device, it was easy to squeeze at 30% of my maximum grip strength for the whole duration of the exercise.	1	2	3	4	5
9. With the **digital** device, it was easy to squeeze at 30% of my maximum grip strength for the whole duration of the exercise.	1	2	3	4	5
10. I could feel muscle fatigue or muscle aches after the exercise with the **analog** handgrip	1	2	3	4	5
11. I could feel muscle fatigue or muscle aches after the exercise with the **digital** handgrip	1	2	3	4	5
12. The **analog** setup made me feel apprehensive of being in a tight space	1	2	3	4	5
13. The **digital** setup made me feel apprehensive of being in a tight space	1	2	3	4	5

Figure 29: Survey form. The questions aim to compare the digital handgrip with the analog one in order to underline the differences, advantages and disadvantages between both ergometers. The scale goes from 1 (*strongly disagree*) to 5 (*strongly agree*),

3.2 Coronary endothelial function assessment

3.2.1 Image acquisition

As previously described in the background section, a retrospectively gated cardiac cine technique requires to record the ECG signal in order to synchronize the data acquisition and avoid motion artefacts. However due to the characteristics of the MR environment such as gradient switching, radiofrequency interference and magnetohydrodynamic (MHD) effect, it can be challenging to measure the ECG signal. Figure 30 illustrates an example of an ECG signal with visible perturbations caused by the MR acquisition. By incorrectly detecting the ECG signal, the final image quality can be considerably degraded. The problem is exacerbated in patients with severe heart diseases.

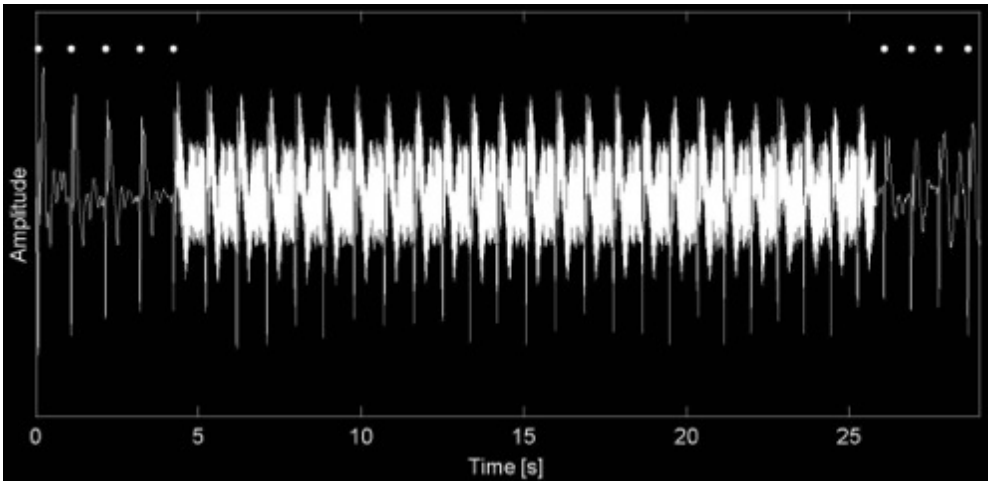

Figure 30: ECG signal using retrospective self-gated technique. In the first 5 seconds, the R-R intervals are possible to detect, but when the data acquisition starts the signal appears completely perturb and the R-R intervals are no longer detectable.

In this thesis, together with the retrospective gating acquisition technique, a self-gating acquisition technique was used in order to eliminate the need of the ECG signal. The self-gating technique derives the trigger/gating times from the image data itself to allow reconstruction of gated-segmented images without the use of ECG. An overview of the self-gated technique is shown in Figure 31. The data were acquired from 11 healthy volunteers after informed consent was obtained on a 3T scanner (MAGNETOM Skyra, Siemens Healthcare) using a free running 2D golden angle radial trajectory (Figure 31a) and a 16-element cardiac coil. The imaging plane was placed perpendicular to a proximal linear segment of the right coronary artery. The relevant imaging parameters include: FOV=260×260 mm^2, base resolution = 416 sample points for each

radial line, pixel size = 0.6×0.6 mm^2, slice thickness = 7 mm, TE/TR = 2.8/5.0 ms, FA = 16˚, breath-hold duration ~ 20 s. To estimate the cardiac self-gating signal, real-time images (Figure 31c) with 37 ms temporal resolution were obtained using a sliding window approach (Figure 31b). These highly undersampled sub-images were reconstructed using a k-t sparse SENSE model (see the background section) with wavelet ant total variation as spatial and temporal regularization terms [42]. From these sub-images, we then selected two reference frames, one in systole and one in late diastole (Figure 31c), and computed the Pearson correlation coefficient (Figure 31d) with all sub-images from a user selected region of interest around the heart. An arrhythmia detection algorithm was developed to analyze both correlation signals and reject radial profiles of cardiac cycles that did not exhibit regularly alternating systolic and diastolic peaks. The systolic correlation signal was then used to retrospectively reorder the radial profiles into cardiac phases (Figure 31e) and the self-gated cine images with high temporal (23 ms) and spatial resolution were reconstructed using the above mentioned k-t sparse SENSE model (Figure 31f). Functional assessment: Finally, we repeated the self-gated and standard ECG-gated acquisitions with and without isometric handgrip stress, and compared the cross sectional area changes of the right coronary artery (RCA). We also assessed the correlation of trigger time points between self-gating and ECG-gating when available.

The images were acquired both using the restrospective ECG-gated and self-gated techniques, in order to compare them. As mentioned before, ECG triggering is not always possible in all the volunteers due to RF interference. Resrospetcive self-gated technqiue can solve this problem.

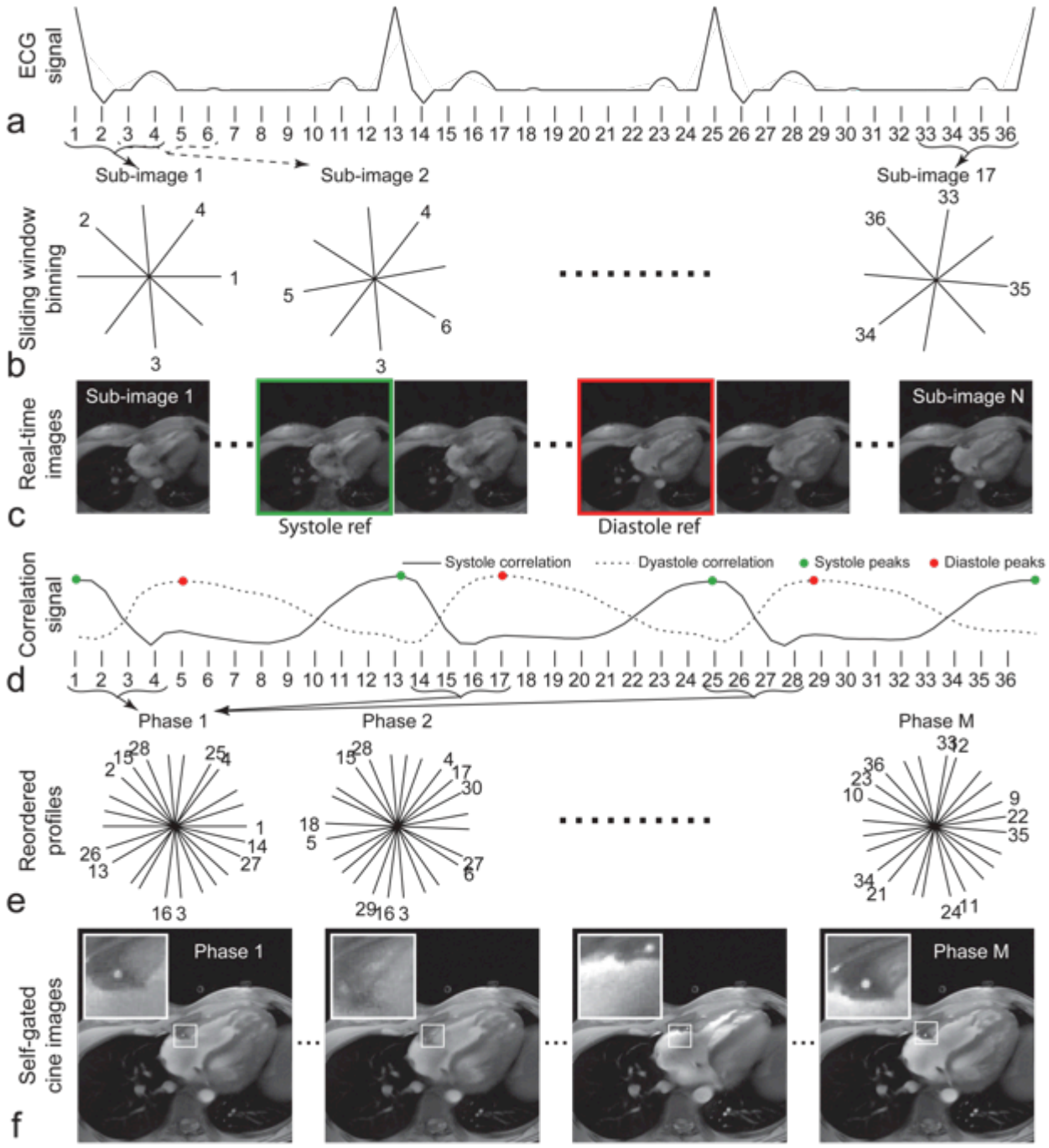

Figure 31: Overview of the self-gated acquisition technique.

3.2.2 Measurement of the cross-sectional area of the coronary artery

After a stress test, a normal vasomotor response of the coronary arteries leads to a vasodilatation of the vessels.[43] In order to quantify the increase in diameter of the coronary artery, the cross-sectional area is measured using a commercial software (Cine Display Application, version 3.5.17 from GE Healthcare) (Figure 32). An objective detection of the border of the coronary artery is automatically obtained by segmenting the vessel lumen using a full-width at half maximum approach or full-width at 75% of maximum approach.
The measurements are performed on the frames where the heart moves the least. For each cine dataset, several measurements were performed on different frames and averaged.

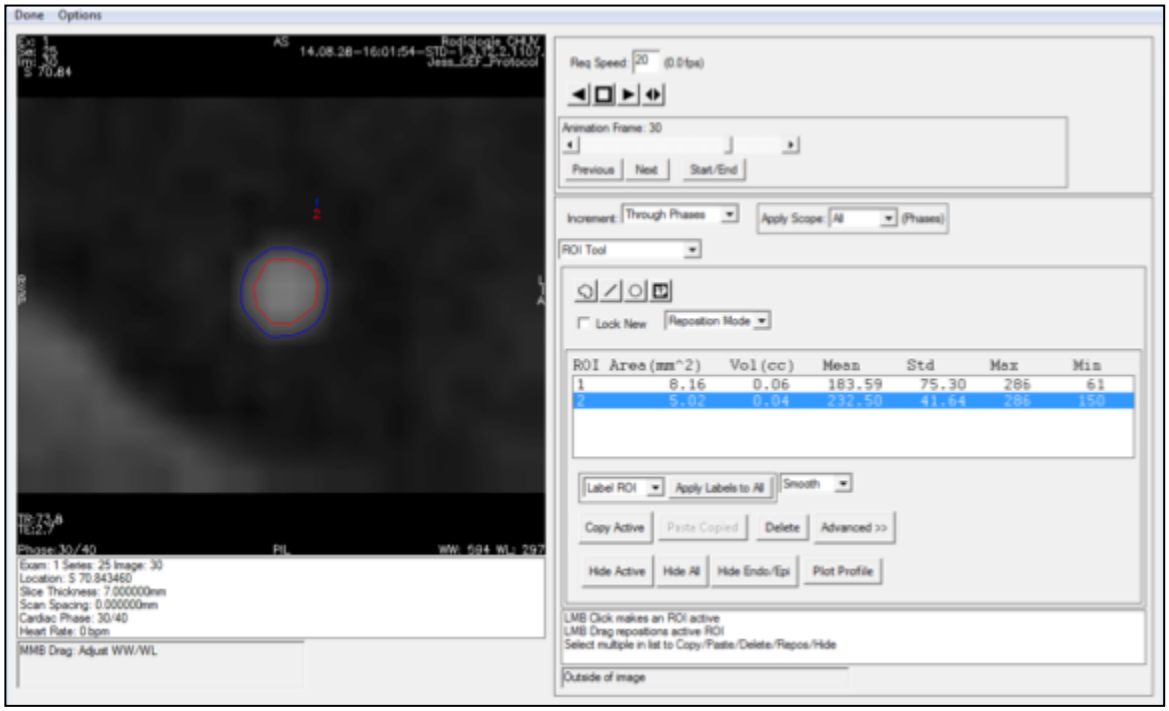

Figure 32: Measurement of the cross-sectional area of the coronary artery using the Cine program. The red circle corresponds to the measurement using a full-width at 75% of maximum approach while the blue one using a full-width at half maximum approach. The only relevant measurement in this study is the area in mm^2

The measurements of the cross-sectional area were both performed on the images acquired with the retrospective ECG-gated and the self-gated imaging techniques. The increase in percentage was compared. The aim is to verify if there is a correlation between the two imaging techniques.

4 Analysis and results

This chapter presents the results obtained by using the implemented handgrip setup with real-time visual feedback. Before actual data acquisition in healthy volunteers, an experiment to verify the linearity of the handgrip has been performed. The obtained results have then been used to make the protocol more accurate. The measurements of the cross-sectional area performed on the images acquired before and after the stress test demonstrate that it is possible to detect a vasodilatation of the coronary artery in response to the isometric handgrip exercise. This chapter presents and discuss these results.

4.1 Protocol for the isometric handgrip exercise

Prior to data acquisition, all the volunteers were asked to squeeze the handgrip at their maximal strength. This value was then recorded and used to personalize the protocol to the subject. In a first version of our protocol, subjects were asked to squeeze the handgrip at 30% of the maximum recorded grip strength during the isometric exercise. This version of the protocol was tested in 7 healthy volunteers. The images were then reconstructed and analysed in order to quantify the coronary artery cross-sectional area. Unfortunately the measurements conducted on these volunteers' cohort, did not show a significant vasodilatation of the coronary artery. We noticed that the heart rate of the volunteers, while they were performing the stress test, was not increasing and thus we supposed that the volunteers were not stressed enough to cause a dilation of the coronaries. To verify our supposition, we designed a test to evaluate the linearity of the handgrip device, which revealed a strong non-linearity. Based on the results of this test, the protocol was then modified. In the new protocol, we increased the requested degree of squeezing from 30% to 40% of the maximum recorded strength of the subject in order to compensate for the non-linearity of the handgrip. With this new protocol, we then performed data acquisition in 4 other volunteers. We noticed that the heart rate increased and the measurements conducted on the coronary artery have shown an increased in cross-sectional area.

4.2 Feedback of the isometric handgrip exercise

Data from a total of 11 healthy volunteers have been collected and analysed. The isometric handgrip exercise consists of two exercises following the same protocol explained in the previous chapter, one exercise performed with the digital handgrip and the second one using the analog handgrip.

The digital handgrip with real-time visual feedback provides a direct evaluation of the grip strength applied by the subject. From the screen of the work station, the operator can see the display that shows the grip strength of the volunteer (Figure 33-a). During the isometric exercise, the grip strength values are collected and recorded in a text file for further analysis and they are plotted as a function of time (Figure 33-b). The plot permits to easily verify whether the volunteer has properly executed the isometric handgrip exercise or not, i.e., he maintained his grip strength within the range of accepted values (green zone in Figure 33)

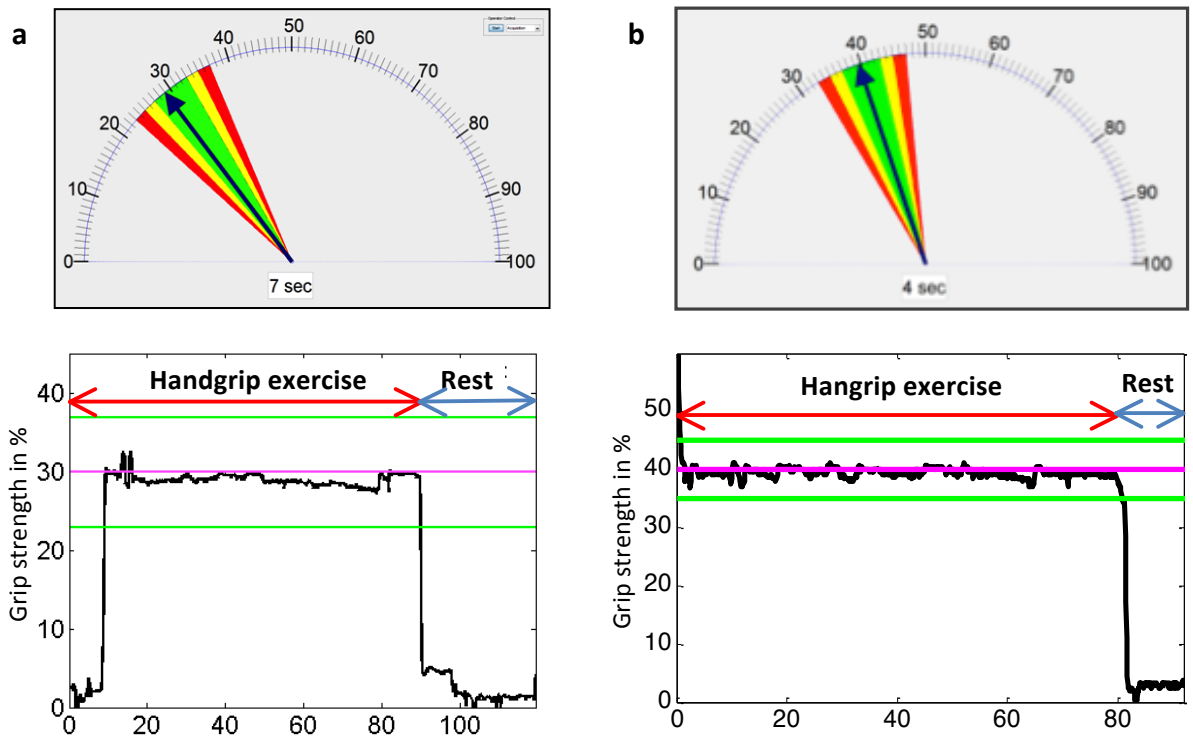

Figure 33: Real-time feedback of the user's grip strength (top row) and plot of the grip strength as a function of time (bottom row) for the 30% squeezing (left column) and for the 40% squeezing (right column). The blue arrow shows the actual grip strength as a percentage of the subject's maximum strength, while the green zone corresponds to the acceptance window.

All the volunteers were capable to maintain the handgrip at 30%±7 and 40%±5, respectively, of their maximal force for the whole duration of the exercise.
The duration of each exercise, both with the analog and digital handgrip, was ~82.2±5.37 seconds.
By summarizing the results from all the surveys in a single graph (Figure 34), it is evident that the digital handgrip makes the isometric exercise easier to perform when compared to the analog handgrip. A particularly interesting result is the one regarding the feeling of the vibrations, which is completely eliminated with the digital ergometer (black bar) compared to the analog one (white bar).

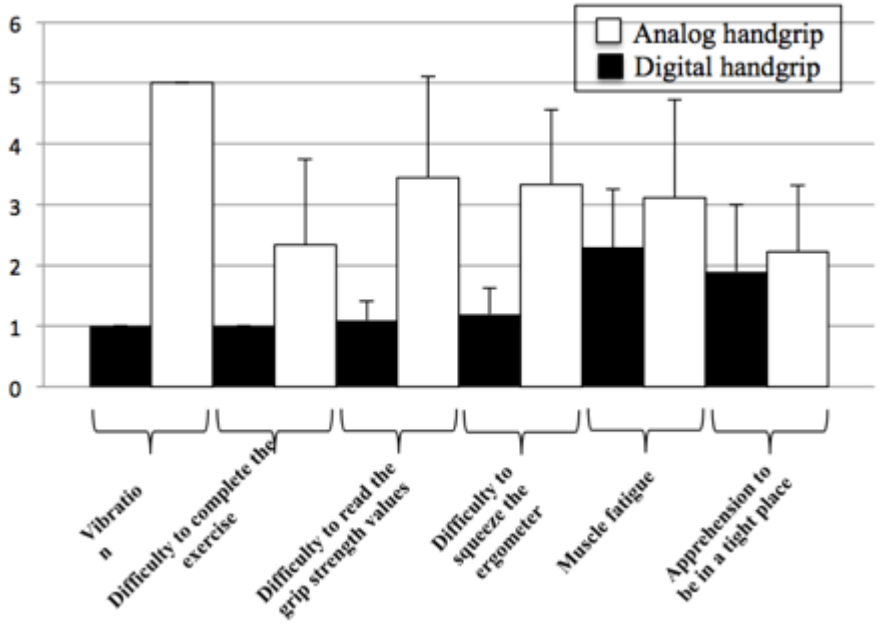

Figure 34: This graph collects the results obtained from the surveys filled up by the volunteers. The x-axis corresponds to the different aspects on which the questions of the survey investigated about, while on the z-axis shows the level of difficulty from 1 (low difficulty) to 6 (high difficulty). The black bars correspond to the digital handgrip while the white bars to the analog handgrip.

4.3 Image acquisition and reconstruction

The cine images were acquired using both the retrospective ECG-gated technique and the retrospective self-gated technique.
The baseline technique, *i.e.* the retrospective ECG-gated technique, uses the ECG signal to trigger the acquisition of the images. Unfortunately it was not possible to correctly detect the ECG signal for all the volunteers because of the interference caused by the rapid switching of the

magnetic field gradients. An incorrect detection of the R peaks of the cardiac cycle results in a wrong synchronization between the data acquisition and the cardiac cycle. Consequently, the final cardiac cine images are not properly synchronized and the coronary artery is no longer visible. Figure 35 shows an image of the coronary artery from a volunteer for whom the ECG was hard to detect, while on the right the image shows the coronary artery of a volunteer for which the ECG was clearly detectable. It is thus evident that an incorrect gating of the ECG can have serious consequences in the final image quality.

a. 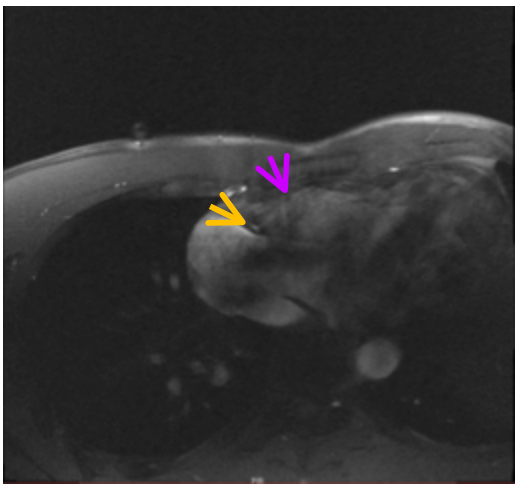 b. 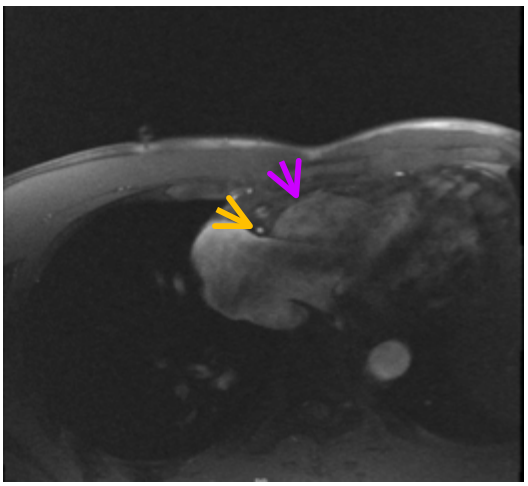

Figure 35: a) The ECG signal of the volunteer was not clearly detectable, thus the coronary artery looks smooth and not well defined (yellow arrow). The borders of the image are also not well defined (purple arrow). b) If the ECG signal of the volunteer can be well detected, then the image quality is improved, with better defined borders (purple arrow) and coronary artery (yellow arrow).

The retrospective self-gated technique is used to avoid this problem. The ECG signal is substituted with a correlation signal and the final cine is obtained by reconstructing the images synchronised with this self-gated signal. Since the ECG signal is no longer necessary, it is always possible to obtain a final reliable cardiac cine.

The advantage of the self-gated approach is more evident in subjects with arrhythmia. The standard ECG approach failed to synchronize the acquisition with the very irregular cardiac cycle and it is impossible to detect the coronary artery as shown in Figure 36.

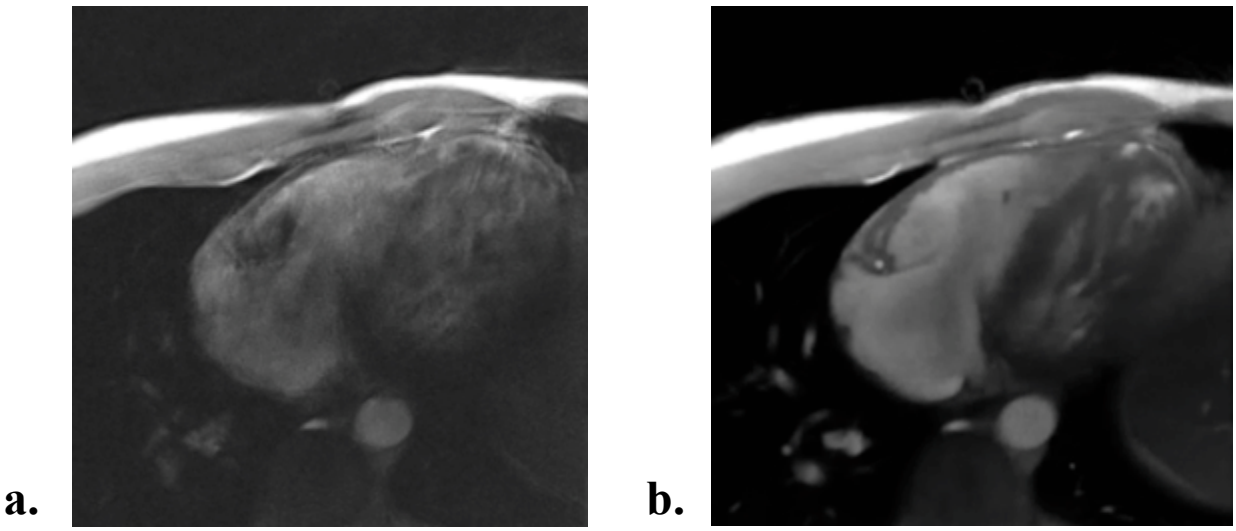

Figure 36: Image obtained using respectively the retrospective ECG-gated technique (a) and the retrospective self-gated technique (b) for a subject with arrhythmia.

4.4 Measurements of the cross-sectional area of the coronary artery before and after the digital handgrip exercise

The quantification of the cross sectional area of the coronary artery were performed on the images acquired for each volunteer before and after the isometric digital handgrip exercise in order to detect a possible dilatation of the vessel due to the stress test. The percentual increment of the dilatation of the coronary artery was measured by computing the cross-sectional area of the coronary artery before and after the exercise.

The program used to measure the cross-sectional area was the automated CINE display application (version 3.5.17) from GE healthcare. The border of the vessel was automatically segmented with a full width at half maximum approach and full width at 75% of half maximum approach. For each volunteer the measurements were done in frames at which the heart was moving the least, usually in diastole, and also where the coronary artery was the most visible and with a round shape. For each volunteer, the average of all the measurements done in the different frames was calculated.

In the following tables (Figure 37), the increase in percentage of the cross-sectional area is shown for each volunteer. The table on the left contains data from the volunteers who performed the isometric handgrip exercise according to the first protocol, i.e., by squeezing at 30% of their maximum grip strength. The table on the right show the data related to the volunteers who followed the second protocol, i.e. by squeezing at 40% of their maximum grip strength. Both tables report the percentages measured on the images acquired with the retrospective-ECG gated

technique and with the retrospective self-gated technique. A positive value indicates vasodilation, and a negative value indicates vasoconstriction.

1.

Increase in % of the vessel lumen, using the first handgrip protocol (at 30%)		
Volunteer	ECG-gated	Self-gated
1	6.83	4.63
2	-0.26	-1.46
3	9.62	9.61
4	7.28	22.92
5	2.94	3.42
6	-11.63	-9.55
7	2.59	5.53

2.

Increase in % of the vessel lumen, using the second handgrip protocol (at 40%)		
Volunteer	ECG-gated	Self-gated
1	11.01	28.33
2	19.07	20.37
3	0.8	4.53
4	8.0	7.14

Figure 37: In table 1 there are the increase percentages of the volunteers that performed the isometric handgrip exercise following the first protocol (with 30% of squeezing), while in table 2 there are the same measurements for the volunteers who performed the exercise with the second protocol.

With the second protocol, *i.e.* with the 40% of the maximal force squeezed, the increase in percentage of the vessel lumen is bigger compared to the one measured using the first protocol (Figure 37). The percentage increase in mean cross-sectional area for the volunteers squeezing at 30% and at 40% was respectively 2.48% ± 7.07 and 9.72% ± 7.56 for the ECG-gated images, 5.01% ± 9.99 and 15.09% ± 11.22 for the self-gated images.

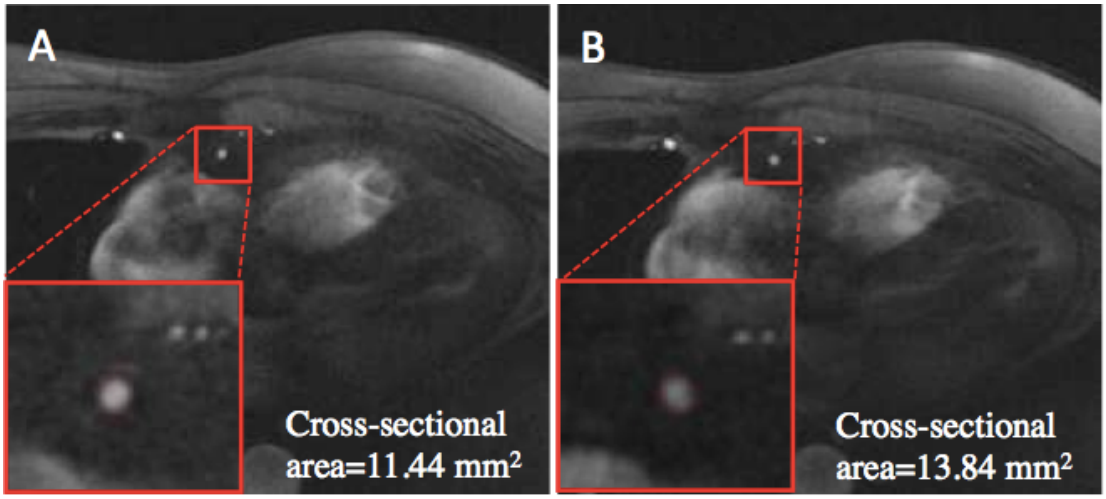

Figure 38: Right coronary artery of a volunteer before (A) and after (B) the isometric handgrip exercise, with the corresponding measurement of the cross-sectional area.

The percentage increase obtained from the self-gated images is slightly bigger than the one calculated in the ECG-gated images. A possible explanation for this result is an improvement in the image quality after reconstruction, which consequently causes improved and more reliable measurements of the cross-sectional area.
The measurements were done both for the images obtained with the baseline and the retrospective self-gated techniques in order to confirm that both techniques are correlated and provide equivalent results (Figure 39). The more reliable measurements obtained with a full width half maximum or with a full width at 75% of half maximum approaches have been used for the final comparison.

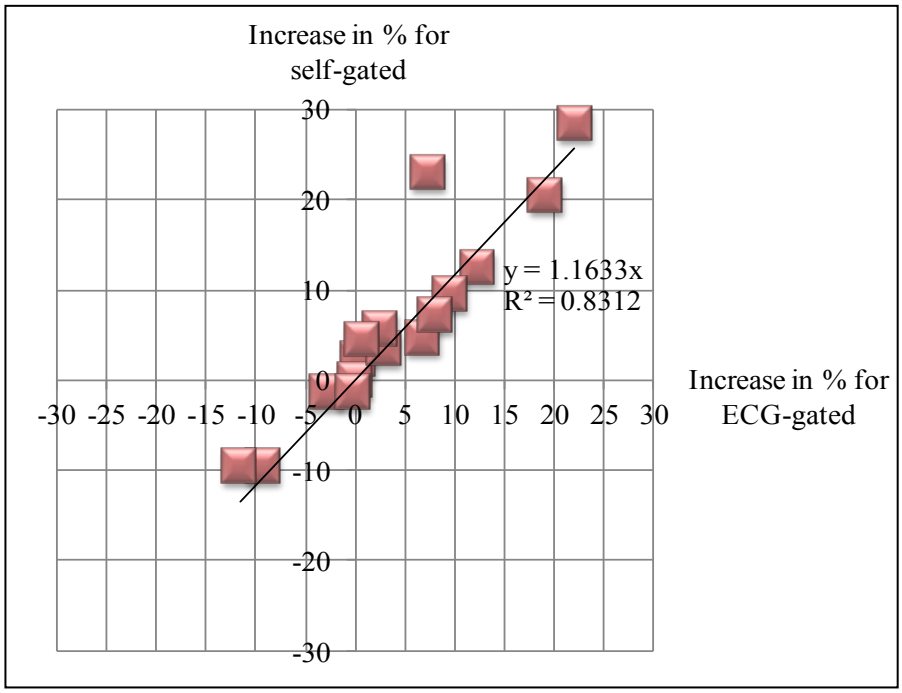

Figure 39: Comparison between the increase percentages obtained from the ECG-gated images and the self-gated images, using the best measurements at full width half maximum or at full width at 75% of the half maximum.

4.5 Test of the linearity of the handgrip response

The response of the handgrip to external applied strength was performed in order to assess the linearity of the device. The measurements were repeated twice and the corresponding handgrip values for both the tests were recorded (see section 3.1.1). The collected data have been then fitted with a third order polynomial equation:

$$y = ax^3 + bx^2 + cx + d$$

After the curve fitting process it is clear that the response of the handgrip is not linear (Figure 40).

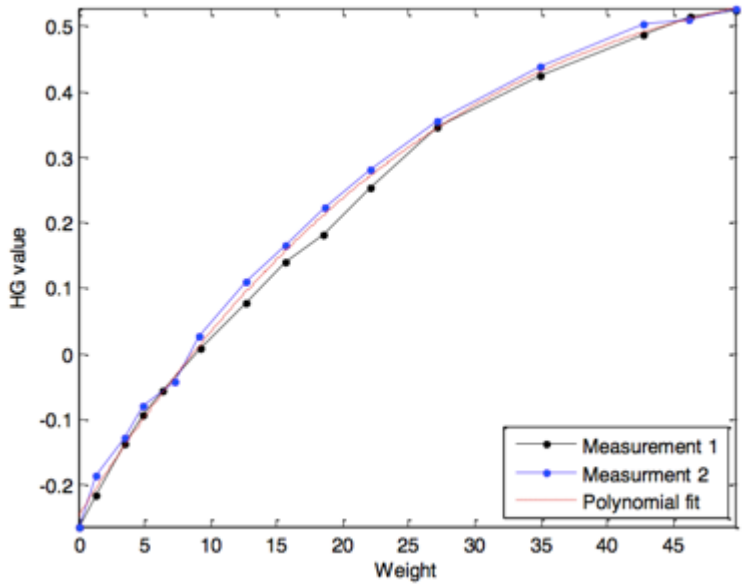

Figure 40:Plot of the two different measurements (black and blue line) and of the corresponding polynomial fit (red line). The curve fitting process permits to find the polynomial equation that better fit the series of data. In this way the data are described through a mathematical model, which can be used to solve the non-linearity of the handgrip response.

By fitting the data with a polynomial curve, it is possible to find the best mathematical model that describes the behavior of the handgrip. This model could be used to correct the non-linearity of the handgrip. Unfortunately, every time the handgrip is reset or turned off, its initial value, *i.e.* the zero value, and consequently the range of the values that the handgrip can have change. Because the baseline and the range of the output values are not constant between sessions, it is not possible to use this mathematical model to correct for the non-linearity of the device.
Thus the results obtained from the linearity test seem to justify the unsatisfactory results obtained by performing the isometric handgrip exercise using the first protocol, i.e. by squeezing at 30%.
Because of the non-linearity of the device, when the volunteers were asked to squeeze at 30% of their maximum grip strength with the first protocol, they were actually only squeezing at about 20% of their maximum grip strength. This explains why we could not detect a significant vasodilation of the coronaries with the first protocol.

5 Conclusions and future work

In this last chapter some conclusions and reflections about the work are proposed. A look to the possible future works is given.

5.1 Conclusions

The aim of this master thesis was to design and develop an entire hardware and software framework to integrate a digital handgrip with MRI for coronary endothelial function assessment.
The digital handgrip has been configured on a 3T MR scanner and the entire set-up has been validated on volunteers. The implemented set-up provides several advantages when compared to the previous analog handgrip. With the new set-up, the volunteers can perform the isometric handgrip exercise without perceiving any vibration of the ergometer device. In addition, the set-up provides a real-time visual feedback of the force exercised on the handgrip during the stress test. This new set-up has been tested and validated in order to assess the coronary endothelial function. The images of the coronary arteries have been acquired before and after the stress test and the change in percentage of the cross-sectional area has been measured. A more evident vasodilatation of the coronary artery has been obtained by using the second protocol, *i.e.* asking the volunteer to squeeze the handgrip at 40% of his maximum grip strength. This can be explained by the non-linear behaviour of the handgrip response, highlighted by the handgrip linearity test. In the first protocol, volunteers were asked to squeeze at 30% of their maximum grip strength, but because of the non-linearity of the handgrip device, the volunteers were actually squeezing at less than 30%, which was most likely not enough to cause a vasodilatation of the vessel.
To conclude, with the implemented and proposed set-up it has been possible to detect an increase of the cross-sectional area of the coronary artery after the isometric handgrip exercise, and the volunteer can easily perform the exercise in a supine and comfortable position, without perceiving anymore the device vibrating

5.2 Future work

The implemented set-up has been validated on healthy volunteers and the results obtained are promising.
The second protocol for isometric handgrip exercise has shown better results compared to the first one but, since the short time available to perform the tests, it has been validated on a small cohort of volunteers. Future works will focus on testing and validating the implemented set-up on a larger cohort of volunteers. After validation, the set-up will be used on a patient population with coronary artery disease. The set-up for isometric handgrip exercise could also be used order to investigate specific diseases, such as diabetes, which has a notable impact on the worldwide healthcare and mortality.
In order to have more detailed assessment of the coronary endothelial function, it would be interesting to support the isometric handgrip exercise with a measurement of the blood pressure together with the heart rate of the patient. This could give additional information regarding the vasomotor response of the coronary artery while the stress test is performed.

5.3 Final reflections

The implemented set-up facilitates the performance of the isometric handgrip exercise inside the MR scanner, since the digital handgrip is no longer affected by eddy currents and the volunteer can lie supine on the MR bed while holding the handgrip in his dominant hand. Since the physical limitations of the previous analog handgrip are now addressed, patients with cardiovascular diseases or any other diseases, who are weaker than healthy volunteers, could easily perform the isometric handgrip exercise. The set-up could then be used in clinical setting in order to investigate specific diseases, and it could be used as a clinical tool in order to investigate an early stage of the disease compared to other diagnostic procedures, such as x-ray coronary angiography.
Consequently this set-up can have an important impact on the healthcare and economy worldwide. The possibility to have a diagnostic tool to detect coronary artery disease at an early stage would allow to intervene before the disease is already at an acute phase, thus reducing the need of additional and heavier therapies and assistance for the patient and consequently reducing the general costs of the healthcare.
By investing in the prevention of cardiovascular events, there is a direct effect on the worldwide mortality, which consequently could decrease.

Set-up for Coronary Endothelial Function Assessment with MR-Compatible Digital Isometric Handgrip and Real-Time Visual Feedback

Giovanna Nordio[1,2,3], Jerome Yerly[1,2], Giulia Ginami[1,2], and Matthias Stuber[1,2]

[1]*Department of Radiology, University Hospital(CHUV) and University of Lausanne (UNIL), Lausanne, Switzerland;* [2]*Center for Biomedical Imaging (CIBM), Lausanne, Switzerland;* [3]*Department of Information engineering, university of Padova, Italy*

Introduction: The endothelium plays a major role in regulating vascular homeostasis by maintaining the correct balance between vasodilatation and vasoconstriction of the vessel wall.[1] Alteration of its normal function can have serious consequences in the development, progression and manifestation of coronary artery disease (CAD).[1] Recent studies have demonstrated that bright blood cine magnetic resonance imaging (MRI) is capable of non-invasively assessing coronary endothelial function (CEF) by measuring the vaso-reactivity of coronaries in response to stress tests, such as isometric handgrip exercise.[2] The handgrip device used in these studies consists of an analog handgrip with an aluminum plate to display the grip strength (Fig. 1).[2-4]This handgrip design, however, has several major drawbacks when used in a MR scanner: (1) the eddy currents induced by the magnetic field cause the device to vibrate, which makes the subject feel uncomfortable, (2) the subject needs to lay prone in the scanner,[2-5] and (3) an external observer is required to continuously monitor subject's grip strength. To address these limitations, we propose a new set-up for isometric handgrip exercise using a digital handgrip integrated with a real-time feedback of user's grip strength. We hypothesize that our proposed set-up provides a more comfortable environment compared to the one with the analog device.

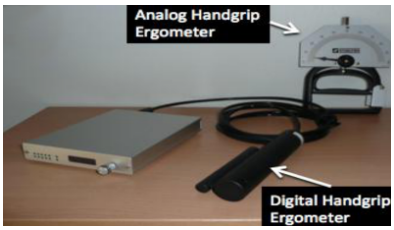

Fig. 41: *Analog and digital handgrip ergometers.*

Methods: Data from 2 healthy volunteers were acquired on a 3T scanner (MAGNETOM Prisma, Siemens Healthcare) using a 2D bright blood cine gradient recalled echo sequence and a 16-element cardiac coil. The imaging plane was placed perpendicular to a proximal linear segment of the right coronary artery. The relevant imaging parameters include: FOV=260×260 mm^2, 320 sample points for each radial line, pixel size = 0.8×0.8 mm^2, slice thickness = 8 mm, and breath-hold duration ~ 20 s. For isometric exercise, a MR-compatible digital handgrip ergometer (Current Design, Inc, PA, USA) (Fig. 1) was connected to a workstation outside the MR room via a fiber optic cable. A custom-written MATLAB (The MathWorks, Inc, Natick, MA, USA) software was implemented to record the handgrip strength and display a real-time visual feedback of the grip strength on a mirror placed at the back of the scanner (Fig. 2b). The subject's maximum grip strength was measured prior to imaging. Images were collected at rest (baseline) and during continuous isometric handgrip exercise at 30±7% of subject's maximal force. Each subject was asked to start the isometric contraction 30 seconds before the actual data acquisition.

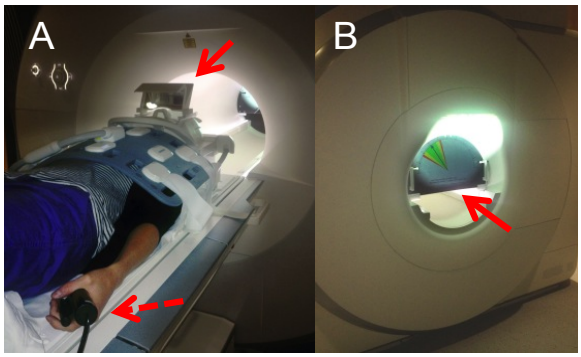

Fig. 2: *Set-up for CEF assessment: isometric digital handgrip (dashed line arrow) integrated with a real-time feedback of user's grip strength (full line arrow).*

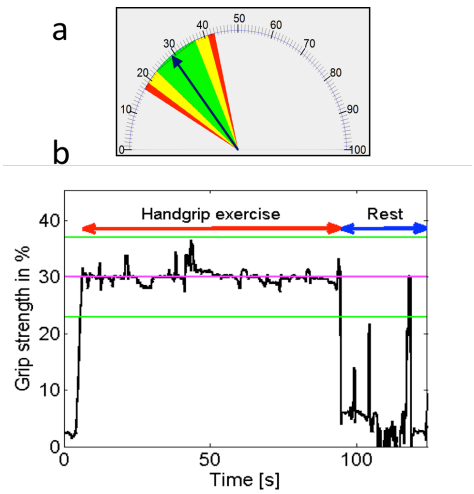

Fig. 3*: a) Real-time feedback of user's grip strength. The blue arrow shows the actual grip strength in % of subject's maximum strength, while the green zone corresponds to the acceptance window (30±7% of maximum grip strength). b) Plot of the grip strength in function of time.*

Results: Cross-sectional images of the RCA were successfully acquired in all volunteers and coronaries were clearly depicted in all images. The subjects performed the handgrip exercise in a supine position (Fig. 2) and reported no handgrip vibration. The real-time visual feedback facilitated precise and reliable control of the grip strength (Fig. 3a). The volunteers were able to maintain their grip strength (29.5±0.7 % of their maximal force) within the acceptance window (green zone in Fig. 3a and 3b) during the whole exercise. Fig. 3b shows the evolution of the grip strength during an isometric handgrip exercise for one of the volunteer.

Discussion: The proposed set-up was successfully tested on healthy volunteers and provides a precise and accurate control of the subject's handgrip strength. Unlike the analog handgrip used in previous studies[2-4], the digital device is not subject to eddy currents. Furthermore, the subject can lay supine in the scanner while observing the mirror for real-time feedback of his grip strength, which prevents the need of an external supervisor inside the MR room. Based on these advantages, we speculate that the proposed set-up can potentially yield more reliable assessment of CEF. Future work will continue to test and validate the proposed set-up in a larger cohort of volunteers.

References: [1] Davignon J. *et al. Circulation* 2004; **109**:III27-32; [2] Hays AG *et al. J Am Coll Cardiol* 2010; **56**:1657-65; [3] Hays AG *et al. Circ Cardiovasc Imaging* 2012; **5**:341-8; [4] Hays AG *et al. PLoS One* 2013; **8**:e58047 [5] Weiss AG *et al. N Engl J Med* 1990; **323**:1593-60

Acknowledgements

This work has been carried out entirely at the Centre for Biomedical Imaging in Lausanne, within the Cardiovascular Magnetic Resonance Group (CVMR) at the University Hospital CHUV of Lausanne.

I would like to thank Professor Matthias Stuber, who gave me the opportunity to work in a stimulating and challenging environment. Thank you to the entire group for the great time we spend together. In particular, thank you Jerome Yerly and Giulia Ginami to support and help me throughout the all project.

I would like to thank Professor Alfredo Ruggeri for mentoring my thesis and to prove to be always helpful during my thesis.

Thank you to my real friends.

And thank you to my dad, my mum and my brother, who sincerely love and support me. You are my life coach and daily benchmark.

REFERENCES

1. Tousoulis, D., M. Charakida, and C. Stefanadis, *Endothelial function and inflammation in coronary artery disease.* Heart, 2006. **92**(4): p. 441-4.
2. Okrainec, K., D.K. Banerjee, and M.J. Eisenberg, *Coronary artery disease in the developing world.* Am Heart J, 2004. **148**(1): p. 7-15.
3. Go, A.S., et al., *Heart disease and stroke statistics--2014 update: a report from the American Heart Association.* Circulation, 2014. **129**(3): p. e28-e292.
4. Melanie Nichols, N.T., Peter Scarborough, Mike Rayner, Jose Leal, Ramon Luengo-Fernandez and Alastair Gray, *European Cardiovascular Disease Statistics*, 2012.
5. Leal, J., et al., *Economic burden of cardiovascular diseases in the enlarged European Union.* Eur Heart J, 2006. **27**(13): p. 1610-9.
6. Insull, W., Jr., *The pathology of atherosclerosis: plaque development and plaque responses to medical treatment.* Am J Med, 2009. **122**(1 Suppl): p. S3-S14.
7. Davignon, J. and P. Ganz, *Role of endothelial dysfunction in atherosclerosis.* Circulation, 2004. **109**(23 Suppl 1): p. III27-32.
8. Botnar, R.M., et al., *Noninvasive coronary vessel wall and plaque imaging with magnetic resonance imaging.* Circulation, 2000. **102**(21): p. 2582-7.
9. Leiner, T., et al., *Magnetic resonance imaging of atherosclerosis.* Eur Radiol, 2005. **15**(6): p. 1087-99.
10. Hays, A.G., et al., *Noninvasive visualization of coronary artery endothelial function in healthy subjects and in patients with coronary artery disease.* J Am Coll Cardiol, 2010. **56**(20): p. 1657-65.
11. Hays, A.G., et al., *Regional coronary endothelial function is closely related to local early coronary atherosclerosis in patients with mild coronary artery disease: pilot study.* Circ Cardiovasc Imaging, 2012. **5**(3): p. 341-8.
12. Hays, A.G., et al., *Non-invasive detection of coronary endothelial response to sequential handgrip exercise in coronary artery disease patients and healthy adults.* PLoS One, 2013. **8**(3): p. e58047.
13. Weiss, R.G., et al., *Regional myocardial metabolism of high-energy phosphates during isometric exercise in patients with coronary artery disease.* N Engl J Med, 1990. **323**(23): p. 1593-600.
14. Gray, H., *Gray's anatomy of the human body.* 1958.
15. Libby, P., *Inflammation in atherosclerosis.* Nature, 2002. **420**(6917): p. 868-74.
16. Tousoulis, D., M. Charakida, and C. Stefanadis, *Endothelial function and inflammation in coronary artery disease.* Postgrad Med J, 2008. **84**(993): p. 368-71.
17. Hansson, G.K., *Inflammation, atherosclerosis, and coronary artery disease.* N Engl J Med, 2005. **352**(16): p. 1685-95.
18. Libby, P., *Inflammation in atherosclerosis.* Arterioscler Thromb Vasc Biol, 2012. **32**(9): p. 2045-51.
19. Costa, J.C.D., *Modern Surgery*. 4th Edition ed1903.
20. Tousoulis, D., et al., *Role of inflammation and oxidative stress in endothelial progenitor cell function and mobilization: therapeutic implications for cardiovascular diseases.* Atherosclerosis, 2008. **201**(2): p. 236-47.
21. Vertes, A. and A. Kali, *[Endothelium-dependent and independent vasodilation in young males with previous myocardial infarction].* Orv Hetil, 2003. **144**(21): p. 1025-9.

22. Fayad, Z.A. and V. Fuster, *Characterization of atherosclerotic plaques by magnetic resonance imaging.* Ann N Y Acad Sci, 2000. **902**: p. 173-86.
23. Abizaid, A.S., et al., *One-year follow-up after intravascular ultrasound assessment of moderate left main coronary artery disease in patients with ambiguous angiograms.* J Am Coll Cardiol, 1999. **34**(3): p. 707-15.
24. Botnar, R.M., et al., *Magnetic resonance coronary lumen and vessel wall imaging.* Rays, 2001. **26**(4): p. 291-303.
25. Lee, N. and T. Hyeon, *Designed synthesis of uniformly sized iron oxide nanoparticles for efficient magnetic resonance imaging contrast agents.* Chem Soc Rev, 2012. **41**(7): p. 2575-89.
26. Donald W. McRobbie, E.A.M., Martin J. Graves and Martin R. Prince, *MRI From Picture to Proton*. Second edition ed, ed. C.U. Press2006.
27. Krishnamurthy, R., B. Cheong, and R. Muthupillai, *Tools for cardiovascular magnetic resonance imaging.* Cardiovasc Diagn Ther, 2014. **4**(2): p. 104-25.
28. Liguori, C., et al., *Dark blood versus bright blood T2 acquisition in cardiovascular magnetic resonance (CMR) for thalassaemia major (TM) patients: evaluation of feasibility, reproducibility and image quality.* Eur J Radiol, 2014. **83**(1): p. e8-e14.
29. Wehrli, F.W., *Time-of-flight effects in MR imaging of flow.* Magn Reson Med, 1990. **14**(2): p. 187-93.
30. Pettigrew, R.I., et al., *MRI techniques for cardiovascular imaging.* J Magn Reson Imaging, 1999. **10**(5): p. 590-601.
31. Terashima, M., et al., *Impaired coronary vasodilation by magnetic resonance angiography is associated with advanced coronary artery calcification.* JACC Cardiovasc Imaging, 2008. **1**(2): p. 167-73.
32. Gibbons, R.J., et al., *ACC/AHA 2002 guideline update for exercise testing: summary article. A report of the American College of Cardiology/American Heart Association Task Force on Practice Guidelines (Committee to Update the 1997 Exercise Testing Guidelines).* J Am Coll Cardiol, 2002. **40**(8): p. 1531-40.
33. Jeneson, J.A., et al., *An MR-compatible bicycle ergometer for in-magnet whole-body human exercise testing.* Magn Reson Med, 2010. **63**(1): p. 257-61.
34. Raman, S.V., et al., *Real-time cine and myocardial perfusion with treadmill exercise stress cardiovascular magnetic resonance in patients referred for stress SPECT.* J Cardiovasc Magn Reson, 2010. **12**: p. 41.
35. von Knobelsdorff-Brenkenhoff, F., et al., *Isometric handgrip exercise during cardiovascular magnetic resonance imaging: set-up and cardiovascular effects.* J Magn Reson Imaging, 2013. **37**(6): p. 1342-50.
36. Gielen, S., et al., *Home-based versus hospital-based exercise programs in patients with coronary artery disease: effects on coronary vasomotion.* Am Heart J, 2003. **145**(1): p. E3.
37. Green, D.J., et al., *Modification of forearm resistance vessels by exercise training in young men.* J Appl Physiol (1985), 1994. **77**(4): p. 1829-33.
38. DESIGNS, C. http://www.curdes.com/. [cited 2014 16 July].
39. Blog, A.-A.C.s. http://algoholic.eu/mat_joy-matlab-interface-for-joysticks/. [cited 2014 21 July].
40. Larson, A.C., et al., *Self-gated cardiac cine MRI.* Magn Reson Med, 2004. **51**(1): p. 93-102.

41. Lustig, M., D. Donoho, and J.M. Pauly, *Sparse MRI: The application of compressed sensing for rapid MR imaging.* Magn Reson Med, 2007. **58**(6): p. 1182-95.
42. Lebel**,** RM, Jones, J, Ferre, J-C, Law, M and Nayak, KS, Highly accelerated dynamic contrast enhanced imaging. *Magn Reson Med,* **71**: 635–644. 2014.
43. Deshmane, A., et al., *Parallel MR imaging.* J Magn Reson Imaging, 2012. **36**(1): p. 55-72.
44. F. Bloch, "Nuclear induction," *Physical Review,* vol. 70, pp. 460-474, 1946.